exhibit aberrant skin epidermis formation, which results in water loss due to incomplete cornified envelope formation (Matsuki et al. 1998).

TG2 is expressed in various cells and tissues and has diverse functions. This enzyme reaction was observed to be involved in cell fate decisions, as determined by its post-translational modifications of extracellular matrix proteins, transcription factors, and signaling molecules (Fesus and Piacentini 2002; Beninati and Piacentini 2004; Mehta et al. 2006; Tatsukawa et al. 2009). Although TG2-null mutants exhibit a normal phenotype at birth, aberrant wound healing, mild glucose intolerance, and abnormal phagocytosis have been observed in the tissues of these mice (Sarang et al. 2009). Celiac disease, related to TG2 activity, has been extensively studied; this disease involves a chronic inflammation of the intestinal mucosa triggered by deamidated gluten-derived peptides (Sollid 2002).

Both of these isozymes have been extensively characterized also in terms of their gene expression and substrate specificity (Esposito and Caputo 2005). However, to better understand their physiological significance, the simultaneous detection of their protein expression and activity patterns in various tissues is essential. To date, the tissue distributions of these proteins and their enzymatic activities have not been thoroughly investigated, particularly during embryonic development.

We have recently identified highly reactive glutamine-donor substrate peptides of TGs using a random 12-mer peptide library (Sugimura et al. 2006, 2008; Hitomi et al. 2009). Because these peptides exhibited a highly selective reactivity to their respective isozymes, these appeared to be an effective tool for detecting the enzymatic activities in an isozyme-specific manner. Generally, the use of a fluorescent-labeled substrate has been an efficient tool for the detection of active enzymes (Van Nooden 2010). Using fluorescent-labeled peptides, for both TG1 and TG2, we successfully detected their specific activities in frozen tissue sections (Sugimura et al. 2008; Akiyama et al. 2010; Yamane et al. 2010; Johnson et al. 2012). When a reaction occurred, a lysine-donor substrate in a tissue section covalently incorporated a glutamine-donor peptide and a fluorescent signal represented apparently the presence of active TGs. In particular, experiments using whole mouse sections efficiently provided the results for the expression levels of TG in the active form (Itoh et al. 2011).

In previous studies, the expression patterns of both TG1 and TG2 were investigated through mRNA expression and protein levels in several tissues (Hiiragi et al. 1999; Griffin et al. 2002). There have been some investigations on the developmental variations of TG expression in some tissues (Nagy et al. 1997; Citron et al. 2000; Bailey and Johnson 2004; Lee et al. 2005). However, variations in these enzymatic activities in whole mice have not been thoroughly investigated, even though both enzymes may be essential for body formation by modifying growth factors and/or by cross-linking several structural proteins. Therefore, to acquire more insights into the physiological roles of these TGs during embryonic development, it is necessary to simultaneously analyze both the protein expressions and the enzymatic activity distributions of TGs.

In this study, we used fluorescent-labeled substrate peptides to determine the mouse embryonic expression pattern of the in situ activities of TG1 and TG2. In addition to detecting their enzymatic activity levels, we simultaneously analyzed and compared their protein distributions using antibodies specific for each isozyme. Our results should contribute to understanding the roles of TG activities during mouse body formation.

Materials & Methods

Materials

Fluorescent isothiocyanate (FITC)-labeled peptides were synthesized by Biosynthesis (Lewisville, TX). Rabbit polyclonal anti-TG1 (A018) was purchased from Zedira (Darmstadt, Germany). Rabbit polyclonal anti-TG2 serum was made by Japan Lamb (Hiroshima, Japan) using mouse recombinant TG2 as an antigen that was produced in our laboratory. IgG was affinity purified using NHS-activated Sepharose 4 Fast Flow, which was immobilized with recombinant protein (GE Healthcare Bio-Sciences AB; Uppsala, Sweden). Alexa 555-labeled donkey anti-rabbit IgG (H+L) and Alexa 594-labeled donkey anti-rabbit IgG (H+L) were purchased from Life Technologies (Carlsbad, CA). MAS coated slide glass was purchased from Matsunami Glass Ind., Ltd. (Osaka, Japan). Other chemical reagents were obtained from Sigma-Aldrich (St Louis, MO) or WAKO Chemicals (Osaka, Japan).

Preparation of Tissue Sections

ICR pregnant mice were purchased from Japan SLC, Inc. (Shizuoka, Japan) and were sacrificed to collect embryos at various pregnancy stages (E10.5, E12.5, E14.5, E16.5, and E18.5). Neonatal mice were also used in this analysis. TG1 and TG2 knockout (KO) C57/BL6 mice were maintained by K. Yamanishi and S. Kojima, respectively. TG2 KO mice were originally developed and kindly provided by Dr. R. Graham (Nanda et al. 2001). Embryos were processed for preparation according to the method described by Kawamoto (Kawamoto and Shimizu 2000; Kawamoto 2003) and whole-body sections were produced using a multipurpose cryosection preparation kit (Section Lab Co. Ltd.; Hiroshima, Japan). Briefly, the mouse was frozen in cold hexane (–94C) and then freeze-embedded with Super Cryoembedding Medium (SCEM). Ten-μm-thick sections were prepared with a cryomicrotome (Leica CM3050S;

Leica Co. Ltd., Wetzlar, Germany) from the frozen specimen block and collected with cryofilm. All sections were histologically identified by hematoxylin and eosin (H&E) staining. Embryonic sequential sections were used for various reactions for in situ enzymatic activity and immunostaining. All animal experiments were carried out according to the guidelines of each institute (Nagoya University, Hyogo College of Medicine, and RIKEN Institute).

In Situ Detection of the Enzymatic Activity of TG

Unfixed 10-μm cryosections of mice embryos were air-dried and then blocked with 1% bovine serum albumin (BSA) in phosphate-buffered saline (PBS; 10 mM Na-phosphate, pH 8.0, 150 mM NaCl) at room temperature for 30 min. These sections were subsequently incubated for 60 min at 37C in the substrate reaction solution containing 100 mM Tris-HCl (pH 8.0), 1 mM dithiothreitol, and 5 mM $CaCl_2$ in the presence of FITC-labeled peptide (pepK5, pepT26) at the final concentration of 1 μM. After the enzymatic reaction, PBS containing 25 mM EDTA was added to stop the reaction via chelating calcium ion. Then, after washing with PBS three times, mounting solution SCMM (R2) was added to the sections for observation. As negative controls, the reaction mixture containing EDTA (5 mM) instead of $CaCl_2$ was used. Alternatively, the fluorescent-labeled peptides (FITC-K5QN or FITC-T26QN) in which the reactive glutamine residue was replaced by an asparagine residue were used in the control reaction.

Immunostaining

Ten-μm cryosections of mice embryos were air-dried and then fixed with mixed solution (methanol:acetone = 1:1) for 1 min. After washing with PBS three times, the sections were blocked with 1% BSA in PBS at room temperature for 30 min. The blocked sections were then incubated with isozyme-specific antibodies diluted 1:250 (anti-TG1) and 1:500 (anti-TG2) in 1% BSA in PBS overnight at 4C. The sections were washed three times with PBS containing 0.15% Triton-X100 and 1% BSA and then incubated for 1 hr at 37C with fluorescent-labeled secondary antibodies: Alexa 555-labeled donkey anti-rabbit IgG (TG1) and Alexa 594-labeled donkey anti-rabbit IgG (TG2), diluted 1:1000 in PBS containing 0.15% Triton-X100 and 1% BSA. After washing with PBS, mount medium was dropped onto the sections for observation.

In the case of double staining, immunostaining was performed followed by in situ enzymatic reactions.

Microscopic Observation and Analyses

Samples were observed under a Keyence fluorescence microscope (BZ-9000; Keyence, Osaka, Japan) using a ×4 lens (NA 0.20) for whole mouse sections and a ×20 lens (NA 0.75) for each tissue. H&E-stained images were obtained using the same microscope or scanner (EPSON GT-x750; Epson, Nagano, Japan).

The free software Image J (version 1.43u; image processing and analyzing java; http://rsbweb.nih.gov/ij/) was used for linear adjustment of fluorescent images. This software was also used for image mapping using pseudo-colors from the fluorescent signal as a standard procedure.

Table 1. Sequences of Isozyme-specific Substrate Peptides for Transglutaminase Skin-type (TG1) (pepK5) and Tissue-type (TG2) (pepT26).

Sequence
TG1: YE**Q**HKLPSSWPF (pepK5)
YE**N**HKLPSSWPF (pepK5QN)
TG2: H**Q**SYVDPWMLDH (pepT26)
H**N**SYVDPWMLDH (pepT26QN)

pepK5QN and pepT26QN are mutant peptides in which the reactive glutamine residue was substituted with asparagine (indicated in bold).

Results

Reactivities and Specificities by Comparative Staining Patterns with Fluorescent-Labeled Favorable Substrate Peptides and Antibodies for TG1 and TG2

To investigate the relationships between the transamidating activities and protein expression levels of TG1 and TG2, we performed both in situ detection of the activity and immunostaining using favorable substrate peptides and antibodies, respectively. The sequences of pepK5 and pepT26 were used to detect TG1 and TG2 activities, respectively, as shown in Table 1. We initially attempted to detect the activities and protein expressions using sections from TG1 and TG2 KO mice as well as wild type mice (Fig. 1). In this figure, sagittal plane sections of an E19.5 embryo and a neonate were used for TG1 and TG2 analyses, respectively. In the case of TG1 analyses, we used E19.5 embryos instead of neonates throughout the experiments, since KO mice for TG1 died within a couple of hours after birth.

For an E19.5 stage wild-type mouse embryo (TG1 +/+), significant fluorescent signals resulting from FITC-labeled pepK5 incorporation were observed in epithelial tissues, which was consistent with our previous results (Itoh et al. 2011). No apparent signals could be detected in a reaction with FITC-pepK5QN substituted peptide or in the co-presence of EDTA. In addition, no signals were observed in a section from a TG1-null mouse. These results demonstrated that active TG1 was specifically detected.

When we used a polyclonal antibody against TG1, signals were obtained in the wild-type section corresponding

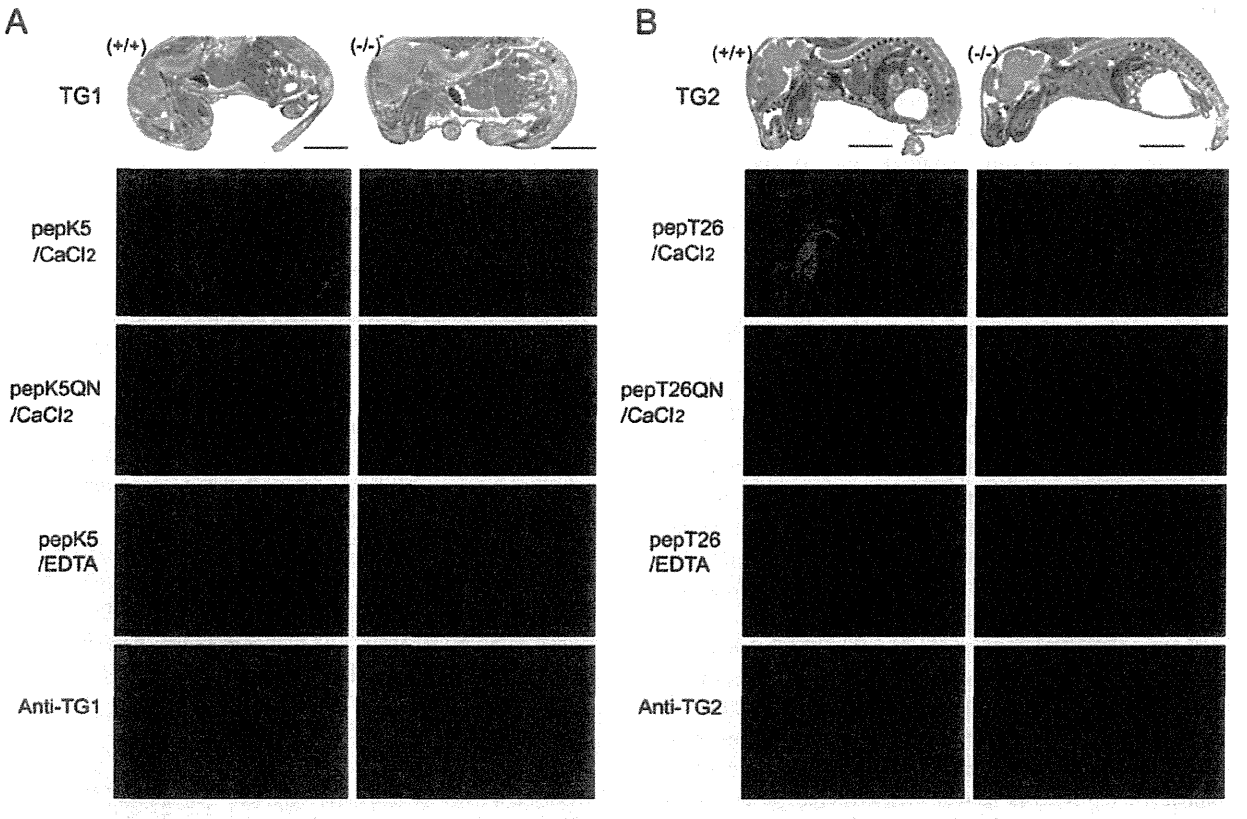

Figure 1. In situ detection of enzymatic activities using the preferential substrate peptides and immunostaining analysis using antibodies against transglutaminase skin-type (TG1) and tissue-type (TG2). (A) Sagittal plane sections from the wild-type and TG1-null mice at E19.5 stage were reacted with 1 μM fluorescent isothiocyanate (FITC)-pepK5 in the presence of 5 mM $CaCl_2$. As negative controls, samples were treated with 1 μM of FITC-pepK5QN or in the presence of 5 mM EDTA. Immunofluorescent staining using a polyclonal antibody against TG1 was also performed. (B) Neonate whole-mouse body sagittal plane sections from wild-type and TG2-null mice were reacted with 1 μM FITC-pepT26. As described in the legend to (A), negative controls (1 μM FITC-pepT26QN or EDTA) and immunostaining with an antibody against TG2 were performed. Bars = 0.5 cm.

to the in situ enzymatic activity of TG1. In contrast, no signals were detected in a section from a TG1-null mouse. In addition, without the primary antibody, no signals were detected in this section (data not shown). These results indicate that these procedures could be used to detect both the enzymatic activity and protein expression.

As shown in Fig. 1B, TG2 activity analysis in wild-type mouse showed significant fluorescent signals that resulted from cross-linked FITC-pepT26 in various tissues, primarily in connective tissues. No apparent signals were observed for a reaction using FITC-pepT26QN substituted peptide or in the co-presence of EDTA. With the exception of tongue and rectum, no apparent signals were observed in a section from a TG2-null mouse. When using a polyclonal antibody against TG2, signals were detected over a wide area with a pattern similar to that for TG2 enzymatic activity. No signals were detected in a section from a TG2-null mouse. These results demonstrated that both TG2 protein expression and the enzymatic activity could be specifically detected using this procedure simultaneously.

Simultaneous Detection of In Situ TG Activity and Protein Expression Patterns in Embryonic Whole Mouse Sections

For this experiment, we performed double-staining analyses of frozen sections from embryos at various developmental stages. Sections that reacted with FITC peptides were subsequently fixed and immunostained. For this immunofluorescent analysis, we used secondary fluorescent-conjugated antibodies for staining. These analyses allowed us to compare the enzymatic activities and protein expression patterns of the two major TGs present in the whole body.

First, for TG1 (Fig. 2B), the results for the detection of in situ enzymatic activity showed significant signals primarily in epithelial tissues, including skin, esophagus, forestomach, and tooth. For these epithelial tissues, an E10.5 section showed weak signals, whereas the E12.5 to E14.5 sections exhibited active signals, particularly around the bronchial arch. These signals were dramatically enhanced at the stage

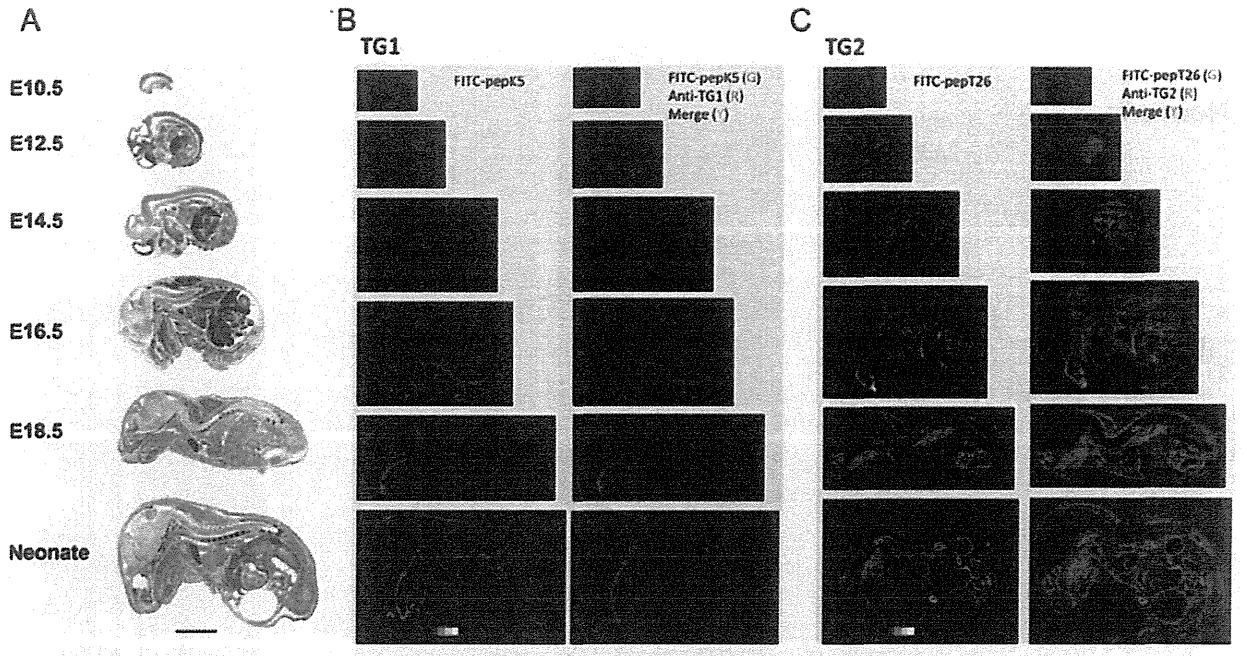

Figure 2. Simultaneous double staining for in situ enzyme activities and immune detection in whole-mouse body sections. (A) Sections of embryos at various fetal development stages (E10.5, E12.5, E14.5, E16.5, E18.5) and neonatal mice were stained with H&E staining. (B) The sections at midline were subjected to in situ enzymatic activity detection [fluorescent isothiocyanate (FITC)-pepK5] followed by immunostaining for transglutaminase skin-type (TG1), using the same reaction conditions described in the legend to Fig. 1. Results in the left panels show enzymatically active areas indicated by pseudo-color images. Results in the right panels show merged areas (yellow) from the stained areas for the enzymatic activity (green) and immunostaining (red). (C) The sections at midline were subjected to in situ enzymatic activity detection (FITC-pepT26) followed by immunostaining for transglutaminase tissue-type (TG2). Results are in the same order as in (B). Bars = 0.5 cm.

of E14.5 to E16.5, as shown by the pseudo-color image data. In a neonate section, signal intensity also began to increase in hair follicles in addition to epithelial areas. Compared with the immunofluorescently stained area, the resulting signals nearly overlapped with those for the signals of active enzyme.

Subsequently, for TG2 (Fig. 2C), the enzymatic activity was particularly higher in liver, heart, and spine compared with other internal organs, on E12.5 to E14.5 sections. An E16.5 section exhibited TG2 activity in other sites, such as muscle. Depending on the developmental stage, the signal pattern gradually changed to reflect that of an adult mouse. With regard to immunofluorescently stained areas, weak enzymatic activity was observed at earlier stages (mostly purple on pseudo-color images). During the embryonic development, the immunofluorescent signals gradually increased.

In Situ Activity and Protein Expression in Specific Tissues

In general, the enzymatic activity level was correlated with the protein expression level. However, in some tissues, the ratios of the levels of enzyme activity and protein levels were varied, as shown by pseudo-color images (Fig. 2). In addition, unique expression patterns were observed in some tissues, as described below (Figs. 3 and 4).

For TG1, which was primarily expressed in skin, the enzyme activity and protein expression levels dramatically increased starting at the E14.5 to E16.5 stage (Fig. 3A). In the outermost cornified layers in the epidermis of the neonate, the immunostaining signal levels were higher than those for enzymatic activity as compared with the patterns in other areas. A similar area (red) was also observed in an E16.5 section, although it was thinner than that in the neonate. This suggested that inactive TG1 itself had possibly accumulated as a substrate in the differentiated keratinocytes by cross-linking. In the neonate, hair follicles also showed apparent signals for TG1 activity and protein expression. Tooth tissues also showed that TG1 was highly expressed in an active form (Fig. 3B). At the E18.5 stage, TG1 activity, which was higher than that of the protein level, was observed around the odontoblast. From the E18.5 stage to the neonatal stage, the protein expression level gradually increased over a wide area containing dentin.

As shown in Fig. 4A, TG2 activity was observed in the cartilage anlagen in the spine at the E12.5 stage. At E14.5, these signals were concentrated in the perichondrium.

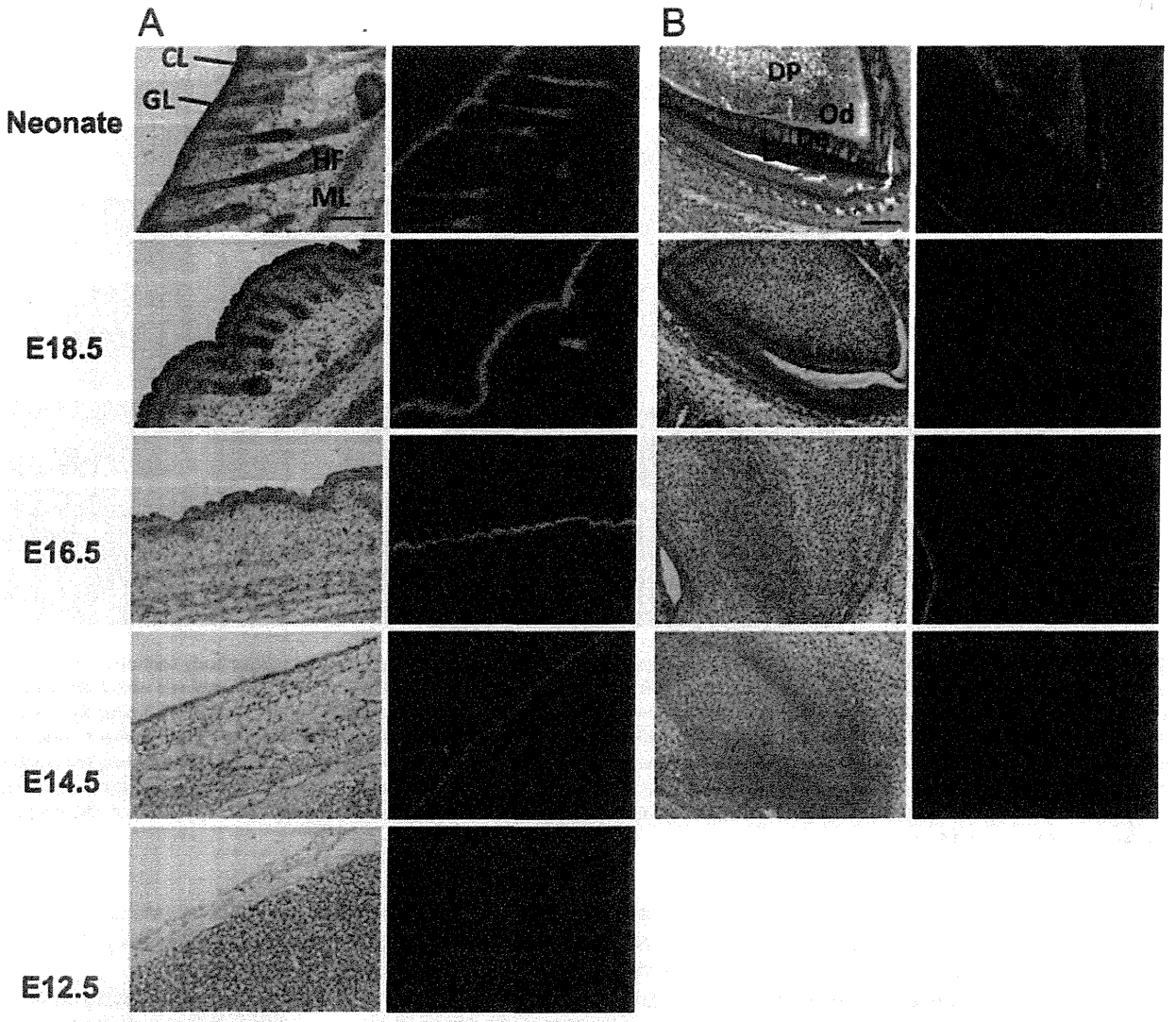

Figure 3. Double-staining patterns for transglutaminase skin-type (TG1) in various tissues during mouse embryonic development. Enlarged pictures of H&E staining (left) and merged images of in situ activities and immunostaining for TG1, using fluorescent isothiocyanate (FITC)-pepK5 and an anti-TG1 antibody (right), are shown. Results in panels A and B are for the reactions with (A) skin and (B) teeth: CL, cornified layer; GL, granular layer; HF, hair follicle; ML, muscle layer; DP, dental papilla; Od, odontoblast; De, dentin; En, enamel. At E14.5 and E16.5, the surrounding area of teeth was shown.

During further development, from the E16.5 stage to the neonatal stage, and between the annulus fibrosus and nucleus pulposus, TG2 activities were enhanced in accordance with the protein levels. In these areas, the protein level was relatively enhanced compared to the enzyme activity. This pattern was also observed in the hyaline cartilage of neonatal nose chondrocytes, whereas the activity relative to protein expression in the perichondrium was increased at a later stage of development (Suppl. Fig.).

In the intestine, in which higher TG2 activity was detected among the tissues, unique expression variations were observed during development (Fig. 4B). At the E12.5 stage, TG2 was highly expressed with regard to its enzymatic activity in the mesenchymal area of the midgut. Regarding villi development, in the intestinal mucosa, TG2 enzymatic activity and the protein level were enhanced in the layers of the lamina propria mucosae, muscularis mucosae, and submucosa.

Discussion

Post-translational modifications by TGs, such as cross-linking between proteins, deamidation, and the attachment of polyamines, are implicated in various biological events. These enzymes, consisting of the eight isozymes, are involved in these reactions in a calcium-dependent manner.

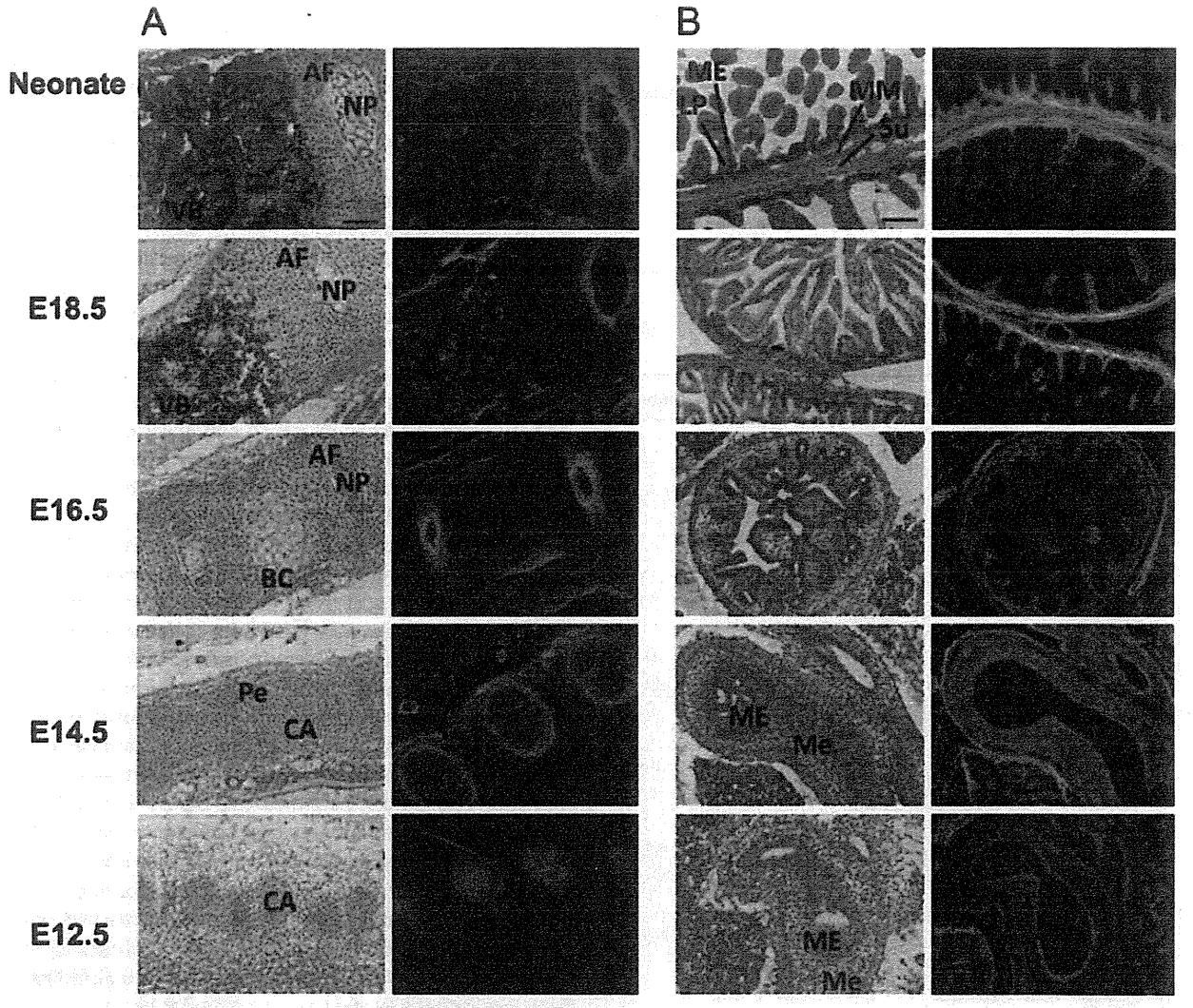

Figure 4. Double-staining patterns for transglutaminase tissue-type (TG2) in various tissues during mouse embryonic development. H&E staining (left) and merged images of in situ activities and immunostaining (right) with corresponding fluorescent isothiocyanate (FITC)-pepT26 and an anti-transglutaminase tissue-type (TG2) antibody are shown. Results in panels A and B are for reactions. (A) Spine: AF, annulus fibrosus; NP, nucleus pulposus; VB, vertebral body; BC, subperiosteal bone collar; Pe, perichondrium; CA, cartilage anlagen. (B) Intestine: ME, mucosal epithelium; LP, lamina propria mucosae; MM, muscularis mucosae; Su, submucosa; Me, mesenchyme. Bars = 100 μm.

Among them, both TG1 and TG2 are major enzymes that are highly expressed in various tissues and have several physiological roles. However, there is little information regarding the distributions of TG activities during embryonic development among these isozymes. Therefore, we aimed to simultaneously acquire insights into the positional and developmental variations in the activities and protein expressions of both TG1 and TG2.

To detect enzymatic activity in an isozyme-specific manner, we established an in situ detection system using fluorescent-labeled peptides that were isozyme-specific glutamine-donor substrates (Itoh et al. 2011). Mouse whole-body sections were successfully prepared for the detection of in situ activities, and these sections also appeared to be suitable for immunostaining analysis (Fig. 1). Furthermore, as shown in Fig. 2, immunostaining analyses could be subsequently performed after detecting the enzymatic activity. Thus, we could compare the protein expression levels and in situ enzyme activities on the same sections, which established precise tissue distributions for TGs (Table 2). In addition, examining various tissues, including tooth, spine, and nose chondrocytes, provided considerably novel information.

Depending on the tissues and embryonic developmental stages, the ratio of the protein level to activity level is varied. In the liver (Fig. 2, neonate) and the intestine at earlier developmental stages (Fig. 4A), the enzyme activity levels relatively increased but the protein levels did not. In these

Table 2. Summary of the Transglutaminase (TG) Protein Expressions and Activity Levels during Mouse Embryo Development.

TG1	E12.5	E14.5	E16.5	E18.5	Neonate
Tongue (epidermis)					
A	-	-	++	++	++
P	+	+	+	++	++
Skin (granular layer)					
A	-	+	++	+++	++
P	-	+	++	++	++
Teeth (odontoblast)					
A	-	-	-	+	+
P	-	-	-	-	+
TG2	**E12.5**	**E14.5**	**E16.5**	**E18.5**	**Neonate**
Tongue (muscle)					
A	-	-	-	+	++
P	-	-	+	++	++
Nose (hyaline cartilage)					
A	+	+	++	++	+
P	-	+	+	++	++
Spine (vertebra body)					
A	+	+	+	++	++
P	-	+	+	++	+++
Heart (myocardial fiber)					
A	++	++	++	++	++
P	++	++	++	++	++
Lung (stroma)					
A	+	+	++	++	+++
P	-	+	++	++	+++
Liver (hepatocyte)					
A	+	+	+	+	+
P	-	-	+	+	+
Intestine (lamina propria mucosae)					
A	+	+	++	+++	+++
P	-	-	++	++	++
Kidney (nephron)					
A	-	+	+	+	+
P	-	-	+	+	+

TG protein expressions and activity levels were classified as either undetectable (-), low (+), intermediate (++), or high (+++). This evaluation was carried out by the human operator's eye. A and P indicate the levels of in situ enzymatic activity and immunologically detected protein, respectively. TG1, transglutaminase skin-type; TG2, transglutaminase tissue-type.

cases, some activation mechanisms may have been required, such as binding of an activator and limited proteolysis in the case of TG1 (Hitomi 2005). In contrast, as observed by the signals in the developed spine and the outermost cornified layers of the skin (Figs. 3A and 3B), the protein levels were higher at these sites than the enzymatic activity levels. In these cases, TG1 may have been a favorable substrate, and participated in cross-linking activity that would result in polymerization and, also possibly, susceptibility to other modifications such as sumoylation and phosphorylation (Luciani et al. 2009; Wang et al. 2012). This would decrease its enzymatic activity, although the area would still be immunochemically positive. Therefore, our data from this study were significant because active enzymes could be detected in each of these tissues.

In a series of experiments from the present and the previous studies, we could not detect enzyme activity in some tissues such as the brain (TG2) and the lung (TG1), where each enzyme is considered to be actively expressed. This was probably because of the release of the cross-linked products, which would make the signal undetectable. Additionally, during preparation of the tissue sections and the cross-linking reaction, which may have led to a loss in cell membrane integrity, limited activity could be detected, such as in the intracellular areas. Further modifications of our procedures will be required in some tissues.

In this study, the signals detected for TG enzymatic activity were based on lysine-donor (glutamine-acceptor) substrates for each TG. Although several TG substrates have been identified, novel substrates may have been included among these signals, in various tissues. Identifying these proteins using tag-attached peptides would enable the biochemical identification of novel substrates, which would be useful information for understanding their physiological significance in each tissue.

In conclusion, we obtained data for the expression patterns of major TGs at both the protein and transamidation activity levels. In addition to our previously developed detection system for in situ enzyme activity, we established conditions to perform a simultaneous immunostaining analysis. Furthermore, reactions for in situ detection of enzyme activity and subsequent immunofluorescent analysis were successfully performed. These analyses provided information on indexes for both enzyme activity and protein expression levels.

Acknowledgments

This work was supported by a Grant-in-Aid for Scientific Research (B) (No. 23380200 to KH; No. 24102533 to SK) and also Grant-in-Aid for Young Scientists Research (No. 24.10612 to MI) from the Ministry of Education, Sports, Science and Technology (JSPS, KAKENHI, Japan) and the Terumo Life Science Foundation (to KH).

Declaration of Conflicting Interests

The author(s) declared no potential conflicts of interest with respect to the research, authorship, and/or publication of this article.

Funding

The author(s) disclosed receipt of the following financial support for the research, authorship, and/or publication of this article: Grant-in-Aid for Scientific Research (B) No. 23380200 (Ministry of Education, Sports, Science and Technology [JSPS], KAKENHI,

Japan); Grant-in-Aid for Young Scientists Research No. 24.10612 (JSPS, KAKENHI, Japan); and the Terumo Life Science Foundation, Japan.

References

Akiyama M, Sakai K, Yanagi T, Fukushima S, Ihn H, Hitomi K, Shimizu H. 2010. Transglutaminase 1 preferred substrate peptide K5 is an efficient tool in diagnosis of lamellar ichthyosis. Am J Pathol. 176:1592–1599.

Bailey CD, Johnson GV. 2004. Developmental regulation of tissue transglutaminase in the mouse forebrain. J Neurochem. 91:1369–1379.

Beninati S, Piacentini M. 2004. The transglutaminase family: an overview. Amino Acids. 26:367–372.

Candi E, Schmidt R, Melino G. 2005. The cornified envelope: a model of cell death in the skin. Nat Rev Mol Cell Bio. 6:328–340.

Citron B, Gregory E, Steigerwalt D, Qin F, Festoff B. 2000. Regulation of the dual function tissue transglutaminase/Gah during murine neuromuscular development: gene and enzyme isoform expression. Neurochem Int. 37:337–349.

Eckert RL, Sturniolo MT, Broome AM, Ruse M, Rorke EA. 2005. Transglutaminase function in epidermis. J Invest Dermatol. 124:481–492.

Esposito C, Caputo I. 2005. Mammalian transglutaminases. Identification of substrates as a key to physiological function and physiopathological relevance. FEBS J. 272:615–631.

Fesus L, Piacentini M. 2002. Transglutaminase 2: an enigmatic enzyme with diverse functions. Trends Biochem Sci. 27:534–539.

Griffin M, Casadio R, Bergamini CM. 2002. Transglutaminases: nature's biological glues. Biochem J. 368:377–396.

Hiiragi T, Sasaki H, Nagafuchi A, Sabe H, Shen SC, Matsuki M, Yamanishi K, Tsukita S. 1999. Transglutaminase type 1 and its cross-linking activity are concentrated at adherens junctions in simple epithelial cells. J Biol Chem. 274:34148–34154.

Hitomi K. 2005. Transglutaminases in skin epidermis. Eur J Dermatol. 15:313–319.

Hitomi K, Kitamura M, Sugimura Y. 2009. Preferred substrate sequences for transglutaminase 2: screening using a phage-displayed peptide library. Amino Acids. 36:619–624.

Itoh H, Kawamoto T, Tatsukawa H, Kojima S, Yamanishi K, Hitomi K. 2011. In situ detection of active transglutaminases for keratinocyte type (TGase 1) and tissue type (TGase 2) using fluorescence-labeled highly reactive substrate peptides. J Histochem Cytochem. 59:180–187.

Johnson KB, Petersen-Jones H, Thompson JM, Hitomi K, Itoh M, Bakker EN, Johnson GV, Colak G, Watts SW. 2012. Vena cava and aortic smooth muscle cells express transglutaminases 1 and 4 in addition to transglutaminase 2. Am J Physiol Heart Circ Physiol. 302:H1355–1366.

Kawamoto T. 2003. Use of a new adhesive film for the preparation of multi-purpose fresh-frozen sections from hard tissues, whole-animals, insects and plants. Arch Histol Cytol. 66:123–143.

Kawamoto T, Shimizu M. 2000. A method for preparing 2- to 50-μm-thick fresh frozen section of large samples and undecalcified hard tissues. Histochem Cell Biol. 113:331–339.

Lee SK, Kim YS, Lee YJ, Lee SS, Song IS, Park SC, Chi JG, Chung SI. 2005. Transglutaminase 2 expression in the salivary myoepithelial cell of mouse embryo. Arch Oral Biol. 50:301–308.

Lorand L, Graham RM. 2003. Transglutaminases: crosslinking enzymes with pleiotropic functions. Nat Rev Mol Cell Biol. 4:140–156.

Luciani A, Villella VR, Vasaturo A, Giardino I, Raia V, Pettoello-Mantovani, D'Apolito M, Guido S, Leal T, Quaratino S, et al. 2009. SUMOylation of tissue transglutaminase as link between oxidative stress and inflammation. J Immunol. 183:2775–2784.

Matsuki M, Yamashita F, Ishida-Yamamoto A, Yamada K, Kinoshita C, Fushiki S, Ueda E, Morishima Y, Tabata K, Yasuno H, et al. 1998. Defective stratum corneum and early neonatal death in mice lacking the gene for transglutaminase 1. Proc Natl Acad Sci USA. 95:1044–1049.

Mehta K, Fok JY, Mangala LS. 2006. Tissue transglutaminase: from biological glue to cell survival cues. Front Biosci. 11:173–185.

Nagy L, Thomazy V, Saydak M, Stein J, Davies P. 1997. The promoter of the mouse tissue transglutaminase gene directs tissue-specific, retinoid-regulated and apoptosis-linked expression. Cell Death Differ. 4:534–547.

Nanda N, Iismaa SE, Owens WA, Husain A, Mackay F, Graham RM. 2001. Targeted inactivation of Gh/tissue transglutaminase II. J Biol Chem. 276:20673–20678.

Sarang Z, Tóth B, Balajthy Z, Köröskényi K, Garabuczi E, Fésüs L, Szondy Z. 2009. Some lessons from the tissue transglutaminase knockout mouse. Amino Acids. 36:625–631.

Sollid LM. 2002. Coeliac disease: dissecting a complex inflammatory disorder. Nat Rev Immunol. 2:647–655.

Sugimura Y, Hosono M, Kitamura M, Tsuda T, Yamanishi K, Maki M, Hitomi K. 2008. Identification of preferred substrate sequences for transglutaminase 1-development of a novel peptide that can efficiently detect cross-linking enzyme activity in the skin. FEBS J. 275:5667–5677.

Sugimura Y, Hosono M, Wada F, Yoshimura T, Maki M, Hitomi K. 2006. Screening for the preferred substrate sequence of transglutaminase using a phage-displayed peptide library: identification of peptide substrates for TGase 2 and Factor XIIIa. J Biol Chem. 281:17699–17706.

Tatsukawa H, Fukaya Y, Frampton G, Martinez-Fuentes A, Suzuki K, Kuo TF, Nagatsuma K, Shimokado K, Okuno M, Wu J, et al. 2009. Role of transglutaminase 2 in liver injury via cross-linking and silencing of transcription factor Sp1. Gastroenterology. 136:1783–1795.

Van Nooden CJF. 2010. Imaging enzymes at work: metabolic mapping by enzyme histochemistry. J Histochem Cytochem. 58:481–497.

Wang Y, Ande SR, Mishra S. 2012. Phosphorylation of transglutaminase 2 at serine-216 has role in TG2 mediated activation of nuclear factor-kappa B and in the down regulation of PTEN. BMC Cancer. 277:1–12.

Yamane A, Fukui M, Itoh M, Alea MP, Thomas V, El Alaoui S, Akiyama M, Hitomi K. 2010. Identification of a preferred substrate peptide for transglutaminase 3 and detection of in situ activity in skin and hair follicles. FEBS J. 277:3564–3574.

THE JOURNAL OF BIOLOGICAL CHEMISTRY VOL. 288, NO. 45, pp. 32720–32730, November 8, 2013

Pituitary Adenylate Cyclase-activating Polypeptide Type 1 Receptor (*PAC1*) Gene Is Suppressed by Transglutaminase 2 Activation*

Received for publication, January 15, 2013, and in revised form, September 13, 2013 Published, JBC Papers in Press, September 17, 2013, DOI 10.1074/jbc.M113.452706

Ayako Miura[‡], Yuki Kambe[‡], Kazuhiko Inoue[‡], Hideki Tatsukawa[§], Takashi Kurihara[‡], Martin Griffin[¶], Soichi Kojima[§], and Atsuro Miyata[‡1]

From the [‡]Department of Pharmacology, Graduate School of Medical and Dental Sciences, University of Kagoshima, Kagoshima 890-8544, Japan, the [§]Molecular Ligand Biology Research Team, Chemical Genomics Research Group, Chemical Biology Department, RIKEN Advanced Science Institute, Wako 351-0198, Japan, and the [¶]School of Life and Health Sciences, Aston University, Birmingham B4 7ET, United Kingdom

Background: The expression of *PAC1*, a specific receptor for PACAP, is decreased in brain ischemia.
Results: *PAC1* expression was attenuated by inactivation of Sp1 through cross-linking by transglutaminase 2 (TG2) activated by ER stress.
Conclusion: TG2 is involved in negative regulation of *PAC1* gene expression.
Significance: Suppression of *PAC1* by TG2 might be involved in neuronal damage from brain ischemia.

Pituitary adenylate cyclase-activating polypeptide (PACAP) functions as a neuroprotective factor through the PACAP type 1 receptor, PAC1. In a previous work, we demonstrated that nerve growth factor augmented *PAC1* gene expression through the activation of Sp1 via the Ras/MAPK pathway. We also observed that *PAC1* expression in Neuro2a cells was transiently suppressed during *in vitro* ischemic conditions, oxygen-glucose deprivation (OGD). Because endoplasmic reticulum (ER) stress is induced by ischemia, we attempted to clarify how ER stress affects the expression of PAC1. Tunicamycin, which induces ER stress, significantly suppressed *PAC1* gene expression, and salubrinal, a selective inhibitor of the protein kinase RNA-like endoplasmic reticulum kinase signaling pathway of ER stress, blocked the suppression. In luciferase reporter assay, we found that two Sp1 sites were involved in suppression of *PAC1* gene expression due to tunicamycin or OGD. Immunocytochemical staining demonstrated that OGD-induced transglutaminase 2 (*TG2*) expression was suppressed by salubrinal or cystamine, a TG activity inhibitor. Further, the OGD-induced accumulation of cross-linked Sp1 in nuclei was suppressed by cystamine or salubrinal. Together with cystamine, R283, TG2-specific inhibitor, and siRNA specific for TG2 also ameliorated OGD-induced attenuation of *PAC1* gene expression. These results suggest that Sp1 cross-linking might be crucial in negative regulation of *PAC1* gene expression due to TG2 in OGD-induced ER stress.

PAC1[2] belongs to the glucagon/secretin family of G protein-coupled receptors. Pituitary adenylate cyclase-activating polypeptide (PACAP) is the high affinity ligand for PAC1. Through PAC1, PACAP plays a crucial role in the central nervous system (CNS) as a neurotrophic factor, neurotransmitter, or neuromodulator (1). PACAP increases the survival of cultured neuronal cells under ischemia-like conditions and has neuroprotective effects in *in vivo* animal models of focal and transient global ischemia (2, 3). It has been reported that after global ischemia, *PAC1* mRNA was decreased throughout the hippocampus in rat, whereas *PACAP* expression was selectively increased in the granule cell layer (4). The expression of *PAC1* has also been shown to decrease after transient focal cerebral ischemia in mice (1). So far, little information has emerged on the reduction of *PAC1* expression in ischemia, and moreover, the mechanism of this suppression remains unclear.

We recently reported that nerve growth factor (NGF) augmented *PAC1* gene expression through the activation of transcription factor Sp1 via the Ras/MAPK pathway in PC12 cells (5). Moreover, it was reported that the administration of Sp1 inhibitor mithramycin A after middle cerebral artery occlusion significantly increased infarct volume in rat (6). Because Sp1 is activated during oxidative stress (7, 8) and hypoxia (9, 10), Sp1 is highly responsive to neuroprotective signals (6).

Endoplasmic reticulum (ER) stress has been reported to contribute to the extent of cerebral infarct volume in ischemic injury (11). ER stress includes a signaling pathway called the unfolded protein response, which is a cellular stress response induced by the accumulation of unfolded proteins in the lumen of the ER. Protein kinase RNA-like endoplasmic reticulum kinase (PERK) receptor response occurs within minutes to hours of unfolded protein response activation to prevent further translational loading of the ER. PERK activates itself by oligomerization and autophosphorylation of the free luminal domain. Although the unfolded protein response is primarily

* This work was supported by Grant-in-aid for Scientific Research 21591182 (to A. M.) from the Ministry of Education, Culture, Sports, Science, and Technology of Japan.

[1] To whom correspondence should be addressed: Dept. of Pharmacology, Graduate School of Medical and Dental Sciences, University of Kagoshima, 8-35-1 Sakuragaoka, Kagoshima 890-8544, Japan. Tel.: 81-99-275-5256; Fax: 81-99-265-8567; E-mail: amiyata@m3.kufm.kagoshima-u.ac.jp.

[2] The abbreviations used are: PAC1, PACAP type 1 receptor; CLSp1, cross-linked Sp1; ER, endoplasmic reticulum; OGD, oxygen-glucose deprivation; PACAP, pituitary adenylate cyclase-activating polypeptide; PERK, protein kinase RNA-like endoplasmic reticulum kinase; TG2, transglutaminase 2; TM, tunicamycin.

an adaptive response, if the stress persists, the ER stress receptors can also trigger pro-apoptotic pathways to initiate cell death (12). Because many proteins synthesized through the ER are glycosylated, tunicamycin (TM), a protein glycosylation inhibitor, induces unfolded protein accumulation in the ER and, ultimately, cell death. Thus, TM is generally used as an inducer in ER stress. Previously, we reported that PACAP protects PC12 cells against TM-induced cell death (13). TM-induced cell death was inhibited by the salubrinal, a selective inhibitor of cellular complexes that dephosphorylates eukaryotic translation initiation factor 2 subunit α (eIF2α) downstream of PERK pathways (14). Moreover, salubrinal significantly increased the phosphorylation of eIF2α, leading to reduced ER stress-induced brain damage after ischemia/reperfusion injury (15).

It has been reported recently that ER stress or ischemia is associated with transglutaminase 2 (TG2; EC 2.3.2.13); that is, TG2 increased in the hippocampus after ischemia (16–18). *TG2* is ubiquitously expressed, and one of its functions is Ca^{2+}-dependent cross-linking of the ϵ-amino group of a lysine residue to the γ-carboxamide group of a glutamine residue (19). TG2 has therefore been implicated in the regulation of cell growth, differentiation, metastasis, and apoptosis. In terms of apoptosis, it was reported that treatment of SH-SY5Y cells with ER stress inducer thapsigargin or TM enhanced the formation of TG2-immunoreactive granules and cell death (20). In addition, alcohol-induced accumulation of TG2 in the nuclei via ER stress induced cross-linking Sp1 and apoptosis in the liver (21, 22), which were inhibited by salubrinal (23). However, it was reported that cystamine, a TG activity inhibitor, exhibits protective effects in brain ischemia and reduces the expression of *TG2* in Neuro2a cells (24).

The purpose of this article is to describe basic data that can be useful to an understanding of the mechanisms of the down-regulation of *PAC1* expression in brain ischemia. We also aimed to clarify a possible mechanism of the down-regulation of PAC1 gene expression via nuclear TG2 in oxygen-glucose deprivation (OGD)-induced ER stress.

EXPERIMENTAL PROCEDURES

Materials—Tunicamycin and cystamine were obtained from Sigma-Aldrich, and salubrinal was from Santa Cruz Biotechnology. Antibodies against GRP78/Bip, CHOP/GADD153, and β-actin were obtained from Santa Cruz Biotechnology; TG2 was from Thermo Scientific; tubulin, fibrillarin, and cleaved caspase-3 were from Cell Signaling Technology; and PAC1 (93093-4) was donated by Dr. Arimura. A polyclonal antibody against cross-linked Sp1 (CLSp1) was prepared as described previously (21). The CLSp1 antibody is designed to recognize the polymerized Sp1 (>450 kDa), but not monomer one. 5-(Biotinamido) pentylamine (5-BAPA), a biotinylated primary amine substrate for TG2, was obtained from Pierce. TG2-specific inhibitor R283 (targeting intracellular TG2) was prepared as described previously (25, 26).

Cell Culture—Neuro2a mouse neuroblastoma cells were maintained in Dulbecco's modified Eagle's medium (DMEM; Sigma) supplemented with 10% fetal bovine serum (FBS). After a 16-h preincubation in DMEM without FBS, the cells were exposed to tunicamycin, salubrinal, cystamine, or R283 for 24 h. Cultures of mouse primary cortical neurons were performed as described previously (27). Briefly, the cortices of embryonic day 15-16 mice were treated with trypsin, and cells were plated on culture dishes at the density of 3×10^4 cells/cm^2. Cells were cultured for 2 h in DMEM supplemented with 10% FBS and then in Neurobasal medium supplemented with 2% B27 supplement (Invitrogen) for up to 21 days *in vitro*. The cells were maintained in a humidified 37 °C incubator with 5% CO_2.

RNA Isolation and RT-PCR—Total RNA was extracted from cells using RNAiso Plus (Takara Bio) according to the manufacturer's protocol. After reverse transcription using a High Capacity cDNA Reverse Transcription Kit (Applied Biosystems), the resulting cDNA was subjected to PCR using TaKaRa Ex *Taq* Hot Start Version (Takara Bio) according to the manufacturer's protocol. PCR conditions were as follows: 30–35 cycles of denaturation at 94 °C for 1 min, annealing at 56 °C for 1 min, and extension at 72 °C for 120 s. The primer sequences were as follows: mouse *PAC1*, 5′-GTGGTGTCCAACTACTTCTG-3′ (forward) and 5′-TGGAGAGAAGGCGAATAC-3′ (reverse); mouse *Sp1* 5′-TCGCTTGCCTCGTCAGCGTC-3′ (forward) and 5′-GCCCACCAGAGACTGTGCGG-3′ (reverse); mouse *GAPDH*, 5′-ACCACAGTCCATGCCATCAC-3′ (forward) and 5′-TCCACCACCCTGTTGCTGTA-3′ (reverse). GAPDH amplification was performed to normalize the results from different samples.

Western Blotting—Western blotting was performed as described previously (5). Briefly, nuclear and cytosolic proteins were extracted from whole cells with NE-PER Nuclear and Cytoplasmic Extraction Reagents (Thermo Scientific) according to the manufacturer's protocol. Each 30 μg of protein was loaded on a 12% polyacrylamide gel for electrophoresis at a constant current of 100 mA/plate for 2 h at room temperature and blotted to a polyvinylidene fluoride membrane previously treated with 100% methanol. After blocking with 5% skimmed milk dissolved in 20 mM Tris-HCl buffer (pH 7.5) containing 137 mM NaCl and 0.05% Tween 20, the membrane was incubated with one of the following primary antibodies: PAC1 (1:5000), Sp1 (1:200), GRP78/Bip (1:1000), CHOP/GADD153 (1:200), TG2 (1:250), cleaved caspase-3 (1:1000), tubulin (1:400), fibrillarin (1:400), or β-actin (1:1000).

OGD Conditions—Neuro2a cells or mouse cortical neurons were washed with phosphate-buffered saline (PBS) once and incubated in DMEM without glucose (11966-025; Invitrogen) after N_2 bubbling for 30 min. The Neuro2a cells or mouse cortical neurons were then incubated in a hypoxia chamber (rectangular jar, 2.5 liters) with an Anaero pack (Mitsubishi Gas Company) to maintain oxygen concentration at <0.1% for 6 h or 1 h, respectively.

Preparation of Vector Constructs for Luciferase Reporter Assays—From the cloned 5′-upstream region of the human *PAC1* gene (*ADCYAP1R1*) (Ensembl Genome Browser: Chromosome7: 31058650–31113403), the fragments were subcloned and inserted into the pGL3 (Promega) as described previously (5). The resulting reporter vectors for *PAC1* promoter activity are designated as hP1L-1, -2, and -3, which contain −372 to +268, −252 to +268, and +23 to +268 of 5′-flanking region of the *PAC1* gene, respectively. The mutated forms at two Sp1 sites of

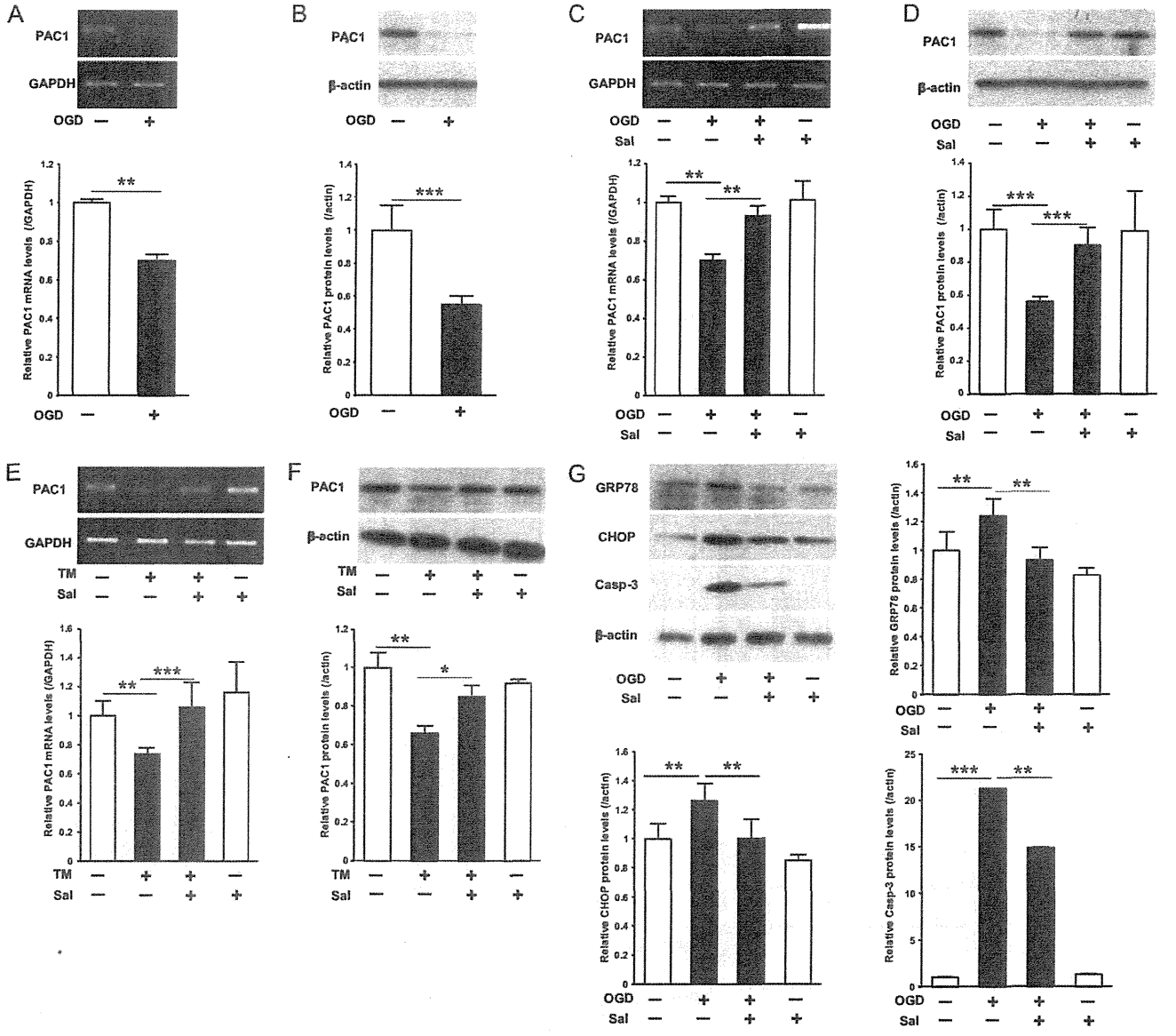

FIGURE 1. **Effect of OGD or TM treatment on *PAC1* expression with or without salubrinal.** Neuro2a cells were treated with OGD for 6 h or with TM for 24 h. *A* and *B*, mRNA (*A*) and protein (*B*) expression of PAC1 after OGD were determined by RT-PCR and Western blotting, respectively. *C* and *D*, mRNA (*C*) and protein (*D*) expression of PAC1 after OGD with presence or absence of salubrinal (*Sal*, 50 μM) were determined. *E* and *F*, mRNA (*E*) and protein (*F*) expression of PAC1 after TM (0.5 μg/ml) treatment with presence or absence of salubrinal were also determined. *G*, after OGD with presence or absence of salubrinal, the protein expression of GRP78, CHOP, cleaved caspase-3, and β-actin in the cytosolic extracts was determined by Western blotting using the specific antibodies. Values are presented as means ± S.E. (*error bars*). *, $p < 0.05$; **, $p < 0.01$; and ***, $p < 0.001$. Representative results from three independent experiments are shown.

hP1L-1 were also prepared using the appropriate synthesized primers with the KOD-Plus-Mutagenesis Kit (Toyobo), as described previously (5). The resulting reporter vectors with mutation of Sp1 elements in −314/−305 and −282/−273 were designated as mut1 and mut2, respectively. The Sp1 element of mut1 (5′-ACCGCGCCCC-3′) and that of mut2 (5′-ACCCCGCCCC-3′) were changed into 5′-ACgaattCCC-3′ and 5′-ACgtcgaCCC-3′, both of which contain a five-point mutation (indicated by lowercase letters) by introducing an EcoRI site and a HincII site, respectively. The Sp1-pGL3 promoter vector, which contains three sequential repeats of consensus GC boxes motifs derived from the c-*met* promoter in the upstream of the luciferase complementary DNA, was generated by inserting a synthesized oligodeoxynucleotide cassette onto the pGL3 vector as described previously (21). All DNAs were prepared using a NucleoBond Xtra Midi EF kit (Macherey-nagel) according to the manufacturer's protocol.

Dual Luciferase Reporter Assay—A dual luciferase reporter assay was performed as described previously (5). Briefly, Neuro2a cells were seeded onto 48-well plates at 1×10^5 cells/well. The cells were co-transfected with mutated vector of hP1L-1, -2, -3, mut1, mut2, or Sp1 with phRL-TK vector using FuGENE 6 (Roche Applied Science) according to the manufacturer's protocol. After the treatment with TM for 24 h, the cells were rinsed with a passive lysis buffer (Promega) for 15 min at room temperature. Luciferase activity was quantified in a Centro

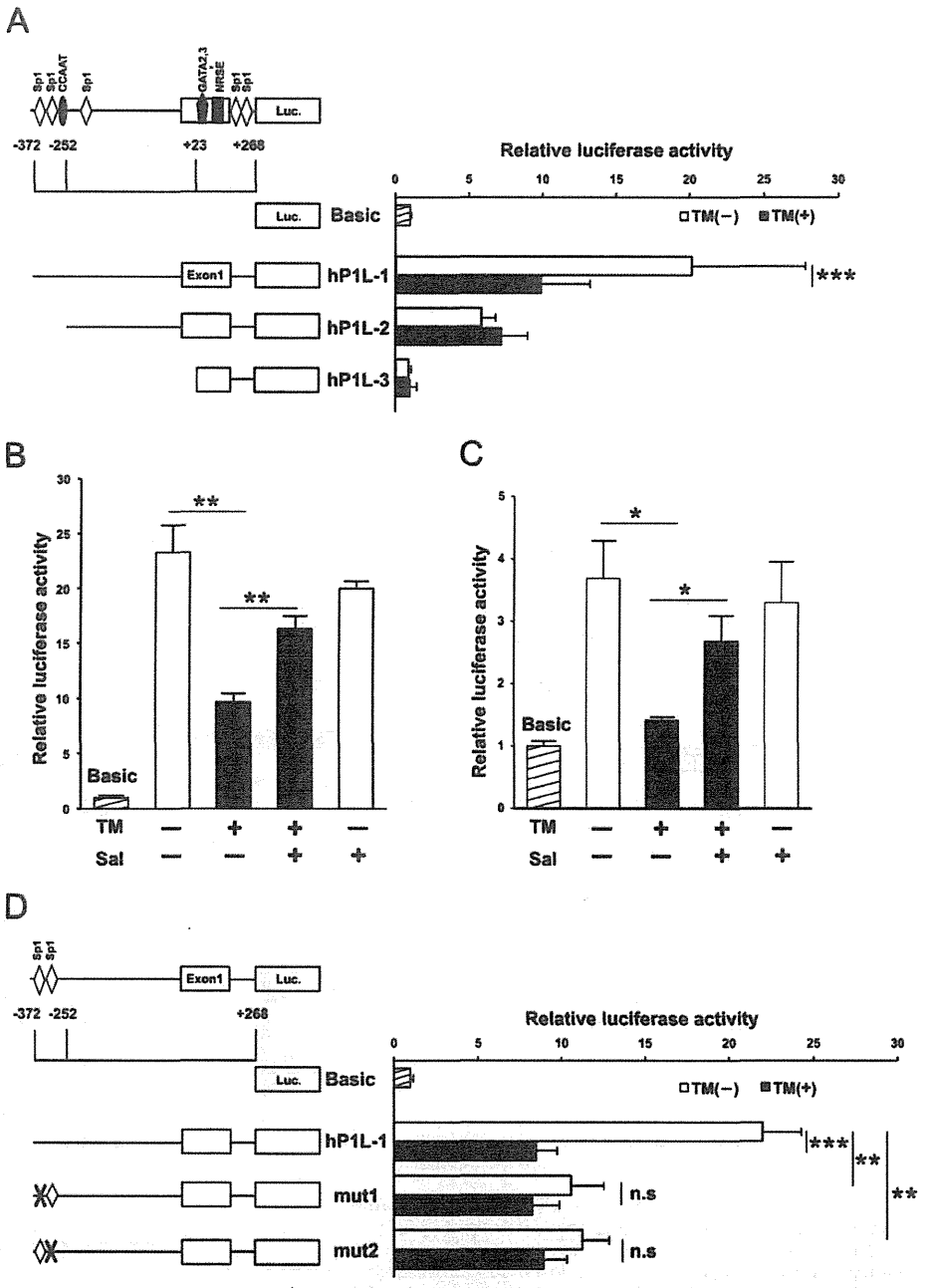

FIGURE 2. **Involvement of Sp1 in suppressive effect of TM on promoter activity of *PAC1* gene.** *A*, luciferase activity of three reporter constructs of the 5′-flanking region of human *PAC1* gene in Neuro2a cells is shown. *B*, after transfection of the reporter vector hP1L-1, Neuro2a cells were treated with TM (0.5 μg/ml) in the absence or presence of salubrinal (*Sal*, 50 μM). *C*, the cells were transfected with Sp1 promoter vector and then treated with TM for 24 h in the absence or presence of salubrinal. *D*, schematic represents the mutated reporter constructs on each Sp1 site, which are designated as mut1 (mutation of Sp1 site in −314/−305 bp) and mut2 (mutation of Sp1 site in −282/−273 bp). Luciferase activities of hP1L-1, mut1, and mut2 were assessed in the TM-treated or nontreated cells. Values are presented as means ± S.E. (*error bars*). *, $p < 0.05$; **, $p < 0.01$; and ***, $p < 0.001$ compared with untreated cells; *n.s.*, not significant. Representative results from three independent experiments are shown.

LB960 (Berthold Technologies) using the Dual Luciferase Reporter Assay system (Promega). Cystamine, TG activity inhibitor, and salubrinal eIF2α dephosphorylation inhibitor were added to the medium 15 min before TM treatment. The relative luciferase activity of the pGL3 promoter was assigned a value of 100.

Immunocytochemistry—Neuro2a or mouse cortical neurons were plated on a coverslip (Matsunami Glass) coated with poly-L-lysine. The cells were fixed for 20 min with 4% paraformaldehyde in PBS, washed with PBS, and incubated in PBS containing 5% bovine serum albumin and 0.3% Triton X-100 for 60 min. Cells were then incubated with antibodies TG2 (1:250) or CLSp1 (2.5 μg/ml) followed by anti-rabbit secondary antibody conjugated with Alexa Fluor 488 (Invitrogen). Samples were mounted on coverslips with Dako mounting medium (Dako Cytomation) containing 0.5 μg/ml Hoechst 33342 (Dojindo Laboratories). Fluorescent images were obtained using an LSM700 confocal laser scanning microscope (Carl Zeiss) and Cellomics™ Arrayscan V system (Thermo Scientific).

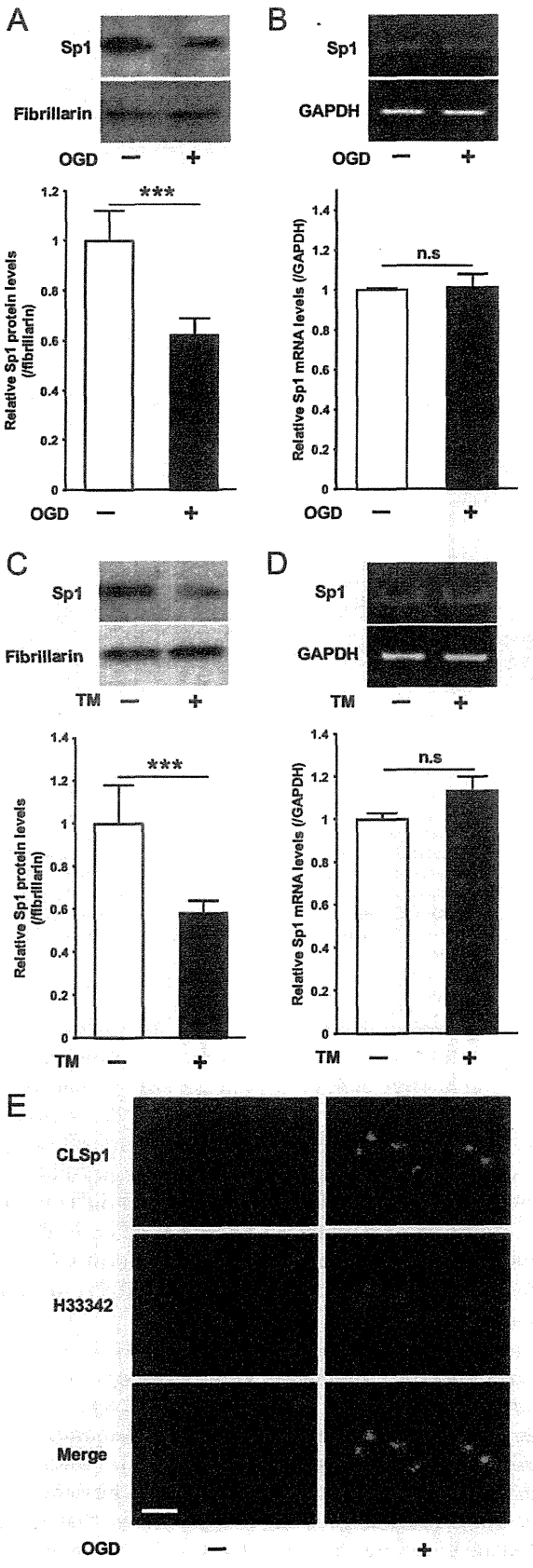

TG2 Activity—*In situ* TG2 activity was assessed as described previously (21, 22). Briefly, *in situ* TG2 activity was detected by incorporation of 5-BAPA into Neuro2a cells. Cells were incubated with 0.2 mM 5-BAPA and 100 μM aminoguanidine for 18 h. After washing with culture medium, cells were fixed, permeabilized, and stained with tetramethylrhodamine isothiocyanate-conjugate streptavidin (1:500).

Short Interfering RNA (siRNA) Transfection—siRNA specific for *TG2* was synthesized by Invitrogen and transfected into Neuro2a cells with Lipofectamine RNAiMAX (Invitrogen) according to the manufacturer's instructions. Briefly, cells were seeded at a density of 0.5×10^5 cells/cm^2 and cultured overnight, after which RNAi/Lipofectamine complexes in Opti-MEM (Invitrogen) were added. After 48 h of incubation, the cells were subjected to OGD as described above. The sequence of *TG2* siRNA oligonucleotides is 5′-GAGCGAGATGATCTGGAAC-3′.

Statistical Analysis—The data are expressed as means ± S.E. Using Prism 5 software (Graph Pad), analyses were performed using Tukey's test after analysis of variance or Student's *t* tests. All experiments were repeated at least three times, and representative results are included in the figures.

RESULTS

OGD or ER Stress Attenuated PAC1 Expression—Because it was previously reported that *PAC1* expression was significantly decreased after experimental ischemic insult *in vivo* (4), we assessed the effect of OGD, a model of ischemic insult *in vitro*, on *PAC1* expression in Neuro2a. The OGD condition decreased *PAC1* mRNA and protein expression levels (Fig. 1, *A* and *B*). Pretreatment with salubrinal ameliorated the suppression of *PAC1* mRNA expression levels (Fig. 1*C*) and that of its protein levels (Fig. 1*D*). As well as OGD, we also found that TM treatment for 24 h decreased the expression of PAC1 protein levels and that salubrinal reversed the suppression of *PAC1* mRNA (Fig. 1*E*) and that of its protein levels (Fig. 1*F*). The expression of ER stress markers CHOP and GRP78 as well as an apoptosis marker, cleaved caspase-3, was increased following OGD, and pretreatment with salubrinal attenuated these expressions (Fig. 1*G*), indicating that ER stress is involved in OGD in Neuro2a cells. Thus, *PAC1* was decreased in OGD-induced ER stress, and pretreatment with salubrinal ameliorated its suppression of *PAC1* expression.

Attenuation of Promoter Activity of PAC1 Gene by Tunicamycin Treatment—Using the dual luciferase reporter assay, we evaluated the influence of ER stress on the promoter activity. Among sequential deletion mutants of the 5′-flanking region, the promoter activity of hP1L-1 was attenuated in

FIGURE 3. **Effect of OGD or TM on *Sp1* expression in Neuro2a cells.** *A* and *B*, after treatment with OGD for 6 h, Neuro2a cells were harvested, and nuclear protein expression (*A*) and mRNA levels of *Sp1* (*B*) were determined by Western blotting and RT-PCR, respectively. *C* and *D*, after treatment with TM for 24 h, the nuclear protein expression (*C*) and the mRNA levels of *Sp1* (*D*) were also determined in the same way. *E*, Neuro2a cells treated with OGD for 6 h were fixed and stained with anti-CLSp1 antibody (*top row*) or Hoechst 33342 (*middle row*). The two images were merged, and the final image is shown in the *bottom row* (*Merge*). ***, $p < 0.001$ compared with untreated cells; *n.s.*, not significant. *Scale bar* (*E*), 20 μm. Representative results from three independent experiments are shown. *Error bars*, S.E.

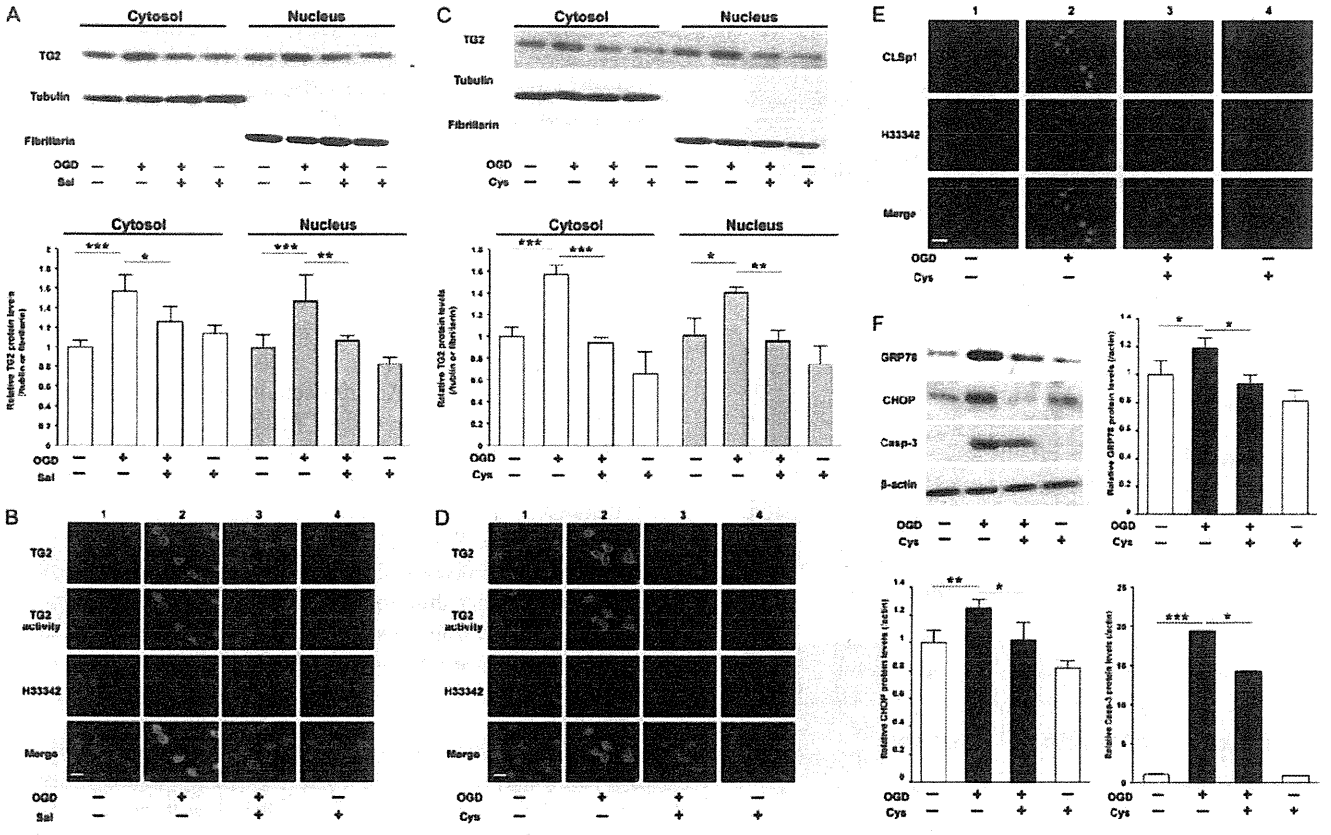

FIGURE 4. **OGD augmented TG2 protein expression in both cytosol and nucleus of Neuro2a cells.** *A*, after treatment of Neuro2a cells with OGD in the absence or presence of salubrinal (*Sal*, 50 μM), the protein levels of TG2, β-tubulin (cytosolic loading control), and fibrillarin (nuclear loading control) in cytosolic and nuclear fractions were determined using Western blotting. *B*, triple staining of TG2 immunoreactivity (*top row*), TG2 activity (*second row*), and Hoechst 33342 (*third row*) after OGD with presence or absence of salubrinal was performed. The results of merging the three images are shown in the *bottom row* (*Merge*). *C*, after treatment with OGD in the absence or presence of cystamine (*Cys*, 500 μM), Western blotting was conducted in the same way. *D*, triple staining of TG2 immunoreactivity (*top row*), TG2 activity (*second row*), and Hoechst 33342 (*third row*) was performed in the OGD-treated cells with or without cystamine. The results of merging the three images are shown in the *bottom row* (*Merge*). *E*, double staining of CLSp1 immunoreactivity (*top row*) and Hoechst 33342 (*middle row*) was performed in the OGD-treated cells with or without cystamine. The results of merging the two images are shown in the *bottom row* (*Merge*). *F*, after OGD treatment with or without cystamine, protein levels of GRP78, CHOP, cleaved caspase-3 (*Casp-3*), and β-actin in cytosolic extracts were determined using Western blotting. Values are presented as means ± S.E. (*error bars*). *, $p < 0.05$; **, $p < 0.01$; and ***, $p < 0.001$. *Scale bars* (*B*, *E*, and *D*), 20 μm. Representative results from three independent experiments are shown.

TM-treated Neuro2a cells (Fig. 2*A*). The treatment with salubrinal significantly reversed the suppression of the promoter activity (Fig. 2*B*). The promoter activity of hP1L-1 was also attenuated in OGD-treated Neuro2a cells (data not shown). Because two Sp1 elements were found between −372 and −252 and ethanol-induced ER stress was reported to suppress Sp1 promoter activity in HepG2 cells, we examined the promoter activity of three tandem functional GC boxes reporter derived from c-*met* gene as described previously (21). As a result, the promoter activity was also significantly decreased by TM treatment, and salubrinal reversed its suppression in Neuro2a cells (Fig. 2*C*). Then a point mutation was introduced at either of two Sp1 elements (−314/−305 bp and −282/−273 bp), designated as mut1 and mut2, respectively. As well as TM treatment, promoter activities of mut1 and mut2 were decreased by insertion of mutation (Fig. 2*D*). Their promoter activities were not changed by treatment of TM. These results suggest that both of putative Sp1-binding elements could be necessary for ER stress-mediated suppression of *PAC1* promoter activity.

Nuclear Cross-linked Sp1 Was Induced by OGD—After 6 h of OGD condition or 24 h of TM treatment, expression levels of Sp1 protein were significantly decreased in Neuro2a cells (Fig. 3, *A* and *C*). *Sp1* mRNA levels, however, were not altered (Fig. 3, *B* and *D*). Based on our previous finding that Sp1 is inactivated by cross-linking in liver injury-induced ER stress (21, 22), we examined whether or not CLSp1 is formed in neurons by OGD-induced ER stress. Then in the OGD condition, immunocytochemical staining with CLSp1-specific antibody demonstrated induction of CLSp1 in nuclei of Neuro2a cells (Fig. 3*E*).

Accumulation of Nuclear Transglutaminase 2 Was Blocked by Salubrinal or Cystamine—We investigated the molecular mechanisms underlying the induction of CLSp1 in Neuro2a cells after OGD. Western blotting analysis demonstrated that OGD increased cytosolic and nuclear TG2 in Neuro2a cells, and salubrinal significantly inhibited these increments (Fig. 4*A*). Immunostaining results also confirmed that OGD-induced nuclear expression and activity of TG2 were suppressed by salubrinal (Fig. 4*B*). It is interesting that cystamine, an inhib-

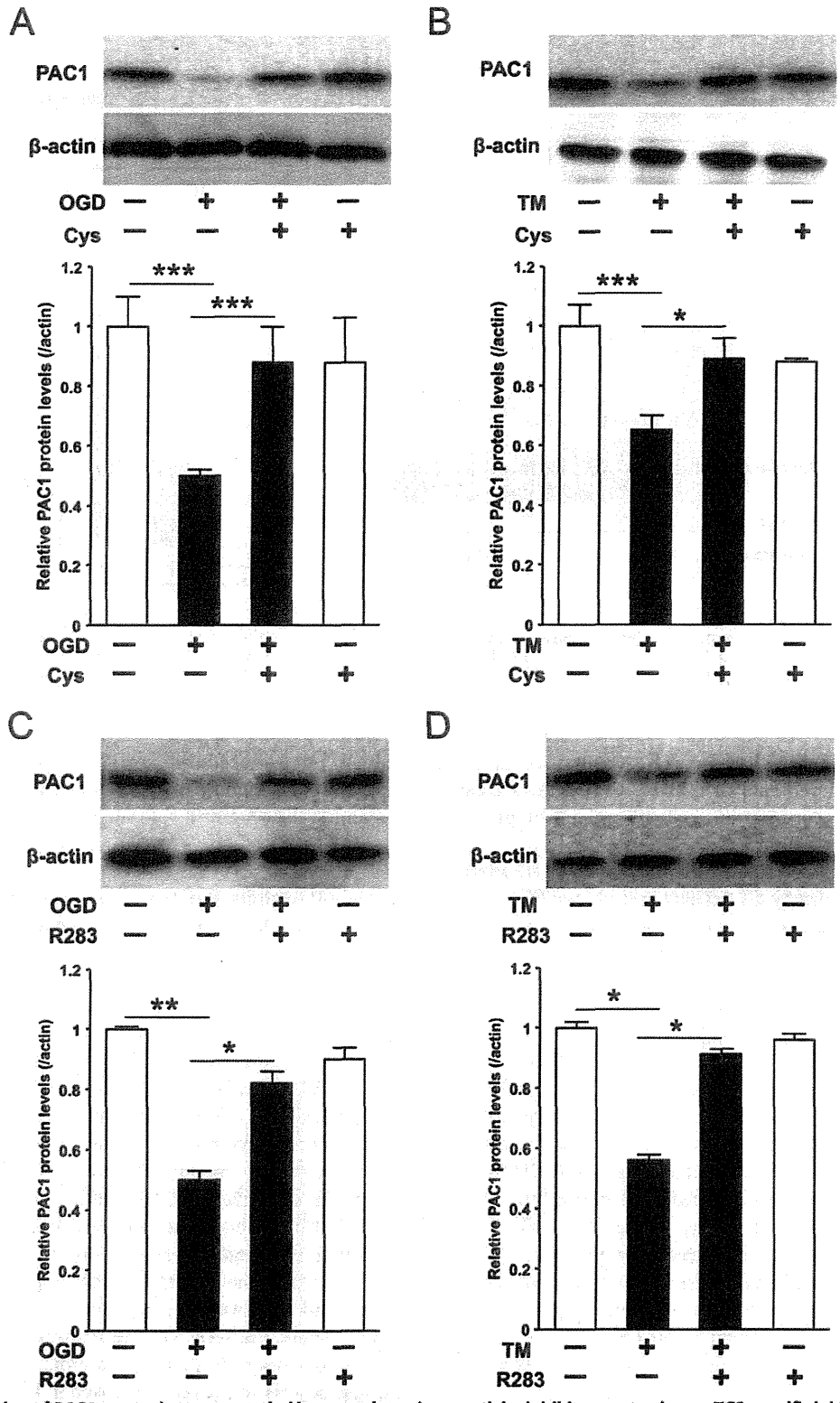

FIGURE 5. **The suppression of *PAC1* expression was canceled by transglutaminase activity inhibitor, cystamine, or TG2-specific inhibitor R283 in Neuro2a cells.** *A* and *B*, the protein expression of PAC1 after OGD or TM treatment with the presence or absence of cystamine (*Cys*, 500 μM) was determined by Western blotting. *C* and *D*, the protein expression of PAC1 after OGD or TM treatment with presence or absence of R283 (25 μM) was determined in the same way. Values are presented as means ± S.E. (*error bars*). *, $p < 0.05$; **, $p < 0.01$; and ***, $p < 0.001$. Representative results from three independent experiments are shown.

itor of transglutaminase activity, significantly inhibited TG2 accumulation in cytosol and nucleus of Neuro2a cells induced by OGD (Fig. 4*C*). Further, as well as salubrinal, OGD-induced nuclear TG2 expression and activity were ameliorated by cystamine (Fig. 4*D*). Immunocytochemical staining demonstrated that the OGD induced accumulation of CLSp1 in Neuro2a

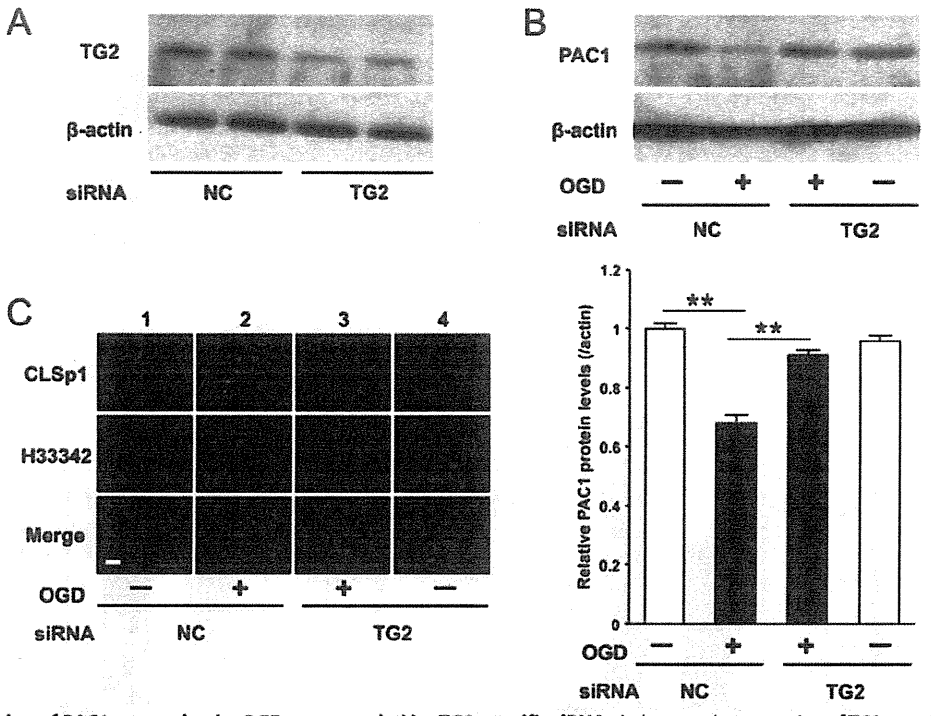

FIGURE 6. **The suppression of *PAC1* expression by OGD was canceled by *TG2*-specific siRNA.** *A*, the protein expression of TG2 was determined by Western blotting after transfection with *TG2*-specific siRNA or negative control (*NC*) siRNA. *B*, the protein expression of PAC1 was also determined after transfection with *TG2*-specific siRNA or negative control. *C*, the cells treated with OGD for 6 h after transfection with TG2-specific siRNA or negative control 1 were fixed and stained with anti-CLSp1 antibody (*top row*) or Hoechst 33342 (*middle row*). The results of merging the two images are shown in the *bottom row* (*Merge*). Values are presented as means ± S.E. (*error bars*). **, $p < 0.01$. *Scale bar* (*C*), 20 μm. Representative results from three independent experiments are shown.

nuclei (Fig. 4*E*, *lane 2*), which was suppressed by cystamine (Fig. 4*E*, *lane 3*). The increments of GRP78, CHOP, and cleaved caspase-3 by OGD were significantly attenuated by pretreatment with cystamine (Fig. 4*F*).

The Suppression of PAC1 Gene Expression by OGD-induced ER Stress Was Canceled by TG Activity Inhibitor or TG2-specific Inhibitor—We attempted to evaluate whether or not TG2 is implicated in TM-induced suppression of PAC1 protein expression. Pretreatment with cystamine significantly ameliorated OGD-induced or TM-induced suppression of *PAC1* (Fig. 5, *A* and *B*). Furthermore, as well as cystamine, TG2-specific inhibitor R283 also canceled the suppression of PAC1 protein expression due to OGD or TM treatment (Fig. 5, *C* and *D*).

Effect of Knocking Down of TG2 on the PAC1 Expression in OGD Ischemia-induced ER Stress—To confirm the involvement of TG2 in the OGD-induced attenuation of *PAC1* gene expression, Neuro2a cells were transfected with siRNA specific for *TG2*, which produced a marked decrease in TG2 protein levels (Fig. 6*A*). Importantly, decreased expression of PAC1 protein by OGD was significantly recovered by the transfection of siRNA against *TG2* (Fig. 6*B*). In addition, the accumulation of CLSp1 in nuclei was abolished by *TG2*-specific siRNA treatment, but not in the cells transfected with control siRNA (Fig. 6*C*).

Effect of OGD Condition or TM Treatment on Primary Mouse Cortical Neurons—OGD significantly decreased *PAC1* mRNA in primary mouse cortical neurons (Fig. 7*A*). Its protein level was also decreased, but was completely recovered by the pretreatment of cystamine (Fig. 7*B*). Both OGD and TM treatment also induced the nuclear expression of TG2 (Fig. 7, *C* and *D*) and induced nuclear accumulation of CLSp1 (Fig. 7, *E* and *F*, *lanes 2*), which was significantly attenuated by pretreatment with cystamine (Fig. 7, *E* and *F*, *lanes 3*).

DISCUSSION

PACAP exhibits pleiotropic action in the CNS through the activation of PAC1. It is well known that both PACAP and NGF enhanced the expression of *PAC1* (1). Zac1, which regulates apoptosis and cell cycle arrest, and *p53*, a tumor suppressor gene, have been shown to induce expression of the *PAC1* gene (28). We have recently demonstrated that NGF augmented *PAC1* gene expression through the activation of Sp1 via the Ras/MAPK pathway in PC12 cells (5). Further, it was reported that PACAP/PAC1 signaling is involved in pathophysiology of post-traumatic symptom disease, in which a human patient demonstrated increments of PAC1 in the amygdala and bed nucleus of the stria terminalis (29). Thus, the positive regulation of PAC1 has been profoundly investigated so far. However, regarding the negative regulation of PAC1, there are few reports, that is, the attenuated expression of PAC1 after transient focal cerebral ischemia in mice (2). Another study reported *PAC1* mRNA was moderately decreased throughout the hippocampus after global ischemia in rat, whereas *PACAP* expression was selectively increased in the granule cell layer of the hippocampus (4). However, the underlying mechanism in the expression of the *PAC1* gene has been unresolved so far. In this context, the data presented here are the first to show a mechanism of decreased *PAC1* expression due to post-transcriptional modification of Sp1, a transcriptional factor responsible for the *PAC1* gene expression, by TG2.

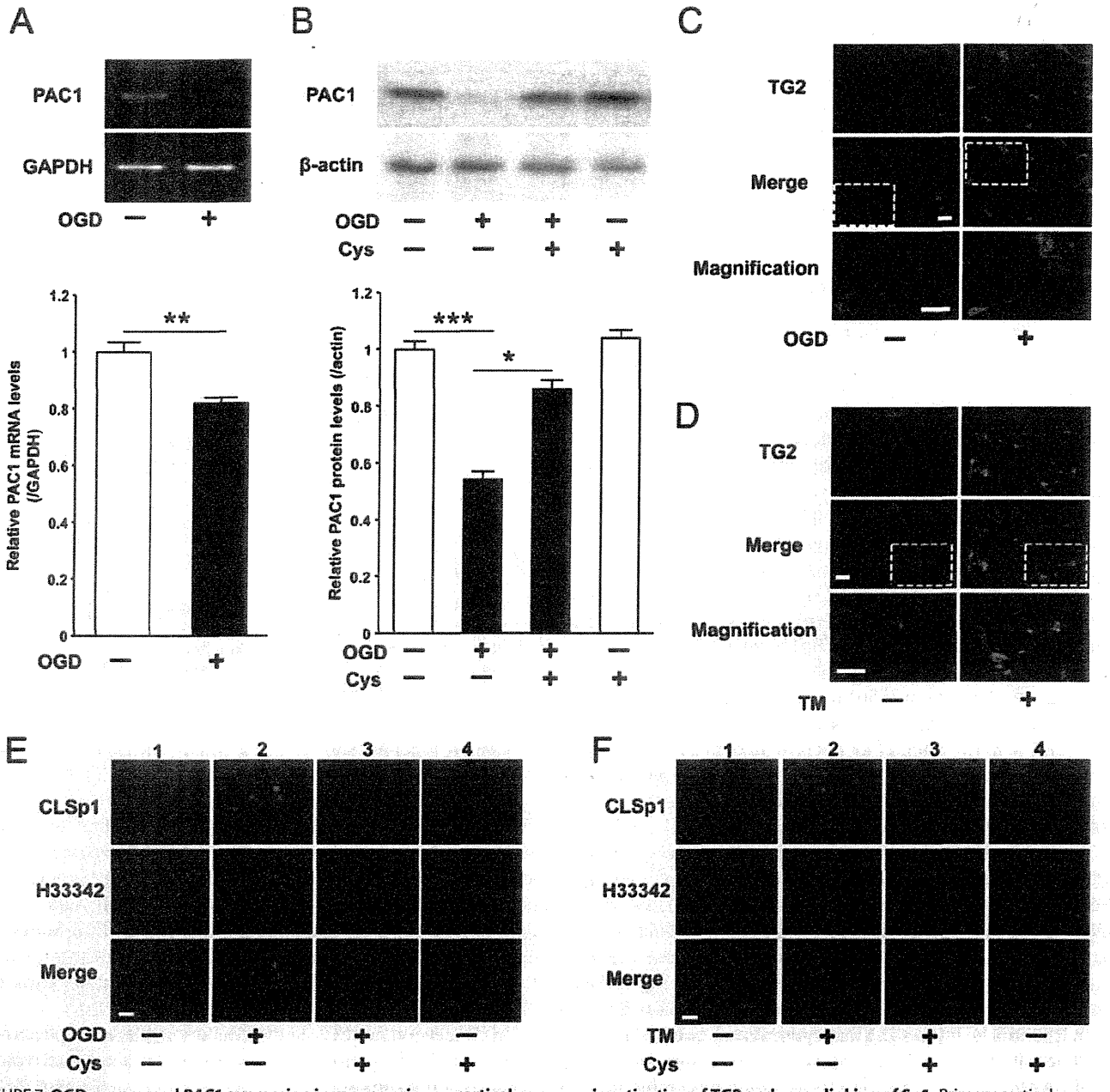

FIGURE 7. **OGD suppressed *PAC1* expression in mouse primary cortical neurons via activation of TG2 and cross-linking of Sp1.** Primary cortical neurons were treated with OGD for 1 h. *A* and *B*, mRNA levels (*A*) and protein expression (*B*) of PAC1 after OGD with presence or absence of cystamine (*Cys*, 250 μM) were determined by RT-PCR and Western blotting, respectively. Values are presented as means ± S.E. (*error bars*). *, $p < 0.05$; **, $p < 0.01$; and ***, $p < 0.001$. Representative results from three independent experiments are shown. *C* and *D*, primary mouse cortical neurons treated with OGD or TM were fixed and stained with TG2 (*top row*). The results of merging the two images, TG2 immunoreactivity and Hoechst 33342, are shown in the *middle row* (*Merge*). The *bottom row* shows double-magnified photographs. *E* and *F*, double staining of CLSp1 immunoreactivity (*top row*) and Hoechst 33342 (*middle row*) after OGD with the presence or absence of cystamine was performed. The results of merging the two images are shown in the *bottom row* (*Merge*). *Scale bars*, 40 μm (*D*) and 20 μm (*E* and *F*).

We first examined how *PAC1* gene expression levels were affected by ER stress with TM or *in vitro* ischemic condition such as OGD. The expressions of cleaved caspase-3, GRP78 as a marker of ER stress and CHOP as an ER stress apoptotic mediator were significantly increased by OGD as well as TM, and their increments were attenuated by salubrinal, indicating a shared mechanism between OGD and TM treatment in terms of ER stress. These findings are also corroborated with previous reports (14). *PAC1* expression levels were potently suppressed by OGD not only in Neuro2a cells but also in primary mouse cortical neurons. Furthermore, salubrinal significantly ameliorated reduction of *PAC1* gene expression by OGD as well as TM, suggesting that the reduction in *PAC1* expression might be primarily due to OGD-induced ER stress.

A luciferase reporter assay was performed to identify which transcriptional element is involved in suppression of *PAC1* gene by ER stress. Among deleted mutants of the 5′-flanking region, the promoter activity of hP1L-1 was most potent and

significantly attenuated by TM treatment in Neuro2a cells, suggesting the presence of responsible element for the gene suppression by TM in the region of −372/−252 bp. Then, a luciferase reporter assay demonstrated that the mutation on each Sp1 site located at −314/−305 bp and −282/−273 bp of hP1L-1 significantly canceled the suppression due to ER stress. The Sp1 site at −282/−273 bp was identical among human, mice, and rat, and the Sp1 site at −314/−305 bp was also almost conserved in all three species, suggesting that these Sp1 sites might be important for the expression of *PAC1* gene. In fact, we recently reported that the Sp1 site at −282/−273 bp was particularly important for NGF-induced expression of *PAC1* gene in PC12 cells (5).

Using Western blot analysis, we found that the protein level of Sp1 was significantly decreased by OGD or TM treatment in Neuro2a cells, although its mRNA level did not change. Based on our previous reports that inactivation and cross-linking of Sp1 have been shown to be induced by TG2 in liver injury-induced ER stress (21, 22), we focused on the cross-linking of Sp1, novel post-transcriptional suppression for protein function, and examined whether OGD-induced ER stress induces the cross-linking of Sp1 in neuronal cells. Immunocytochemical staining showed that the CLSp1 was induced in nuclei under the OGD-induced ER stress and was suppressed by salubrinal, cystamine or R283 (data not shown). This is the first report that inactivation and cross-linking of Sp1 were induced by ER stress in neurons. These data suggest that, in addition to PAC1, cross-linking and inactivation of Sp1 might also impair the expression of Sp1-regulated target genes, which are critical for cell growth and survival in the CNS. Thus, decrement of protein expression but not mRNA expression of Sp1 was due to the cross-linking of Sp1, which contributed to the decrement of the expression of PAC1 underlying ER stress.

Although other reports demonstrated the augmentation of TG2 expression in the hippocampus after reperfusion in a gerbil model of global cerebral ischemia (17, 30, 31), we found OGD-induced ER stress increased expression of TG2 not only in cytosol but also in nuclei of neuronal cells. Then OGD-induced nuclear TG2 expression and TG2 activity were markedly attenuated by salubrinal in agreement with previous findings (23). It should be interesting that cystamine attenuated not only TG2 activity but also TG2 expression, which were induced by OGD. Although cystamine is a transglutaminase inhibitor and its underlying mechanism remains unknown, previous reports also demonstrated the suppression of TG2 expression by cystamine (31, 32). Then by using TG2-specific inhibitor R283 and *TG2*-specific siRNA, we attempted to confirm whether or not TG2 is involved in suppression of PAC1 in OGD-induced ER stress. As a result, both treatments attenuated the accumulation of CLSp1 and the suppression of *PAC1* expression in Neuro2a cells not only by TM treatment but also by OGD. Thus, we provide evidence that the accumulation of TG2 in the nucleus induces the formation of CLSp1, which subsequently suppresses *PAC1* expression under OGD-induced ER stress in neuronal cells.

Regarding the effect on viability of neuronal cells, treatment with either OGD or TM reduced their survival rate, which was significantly ameliorated by the pretreatment with salubrinal or

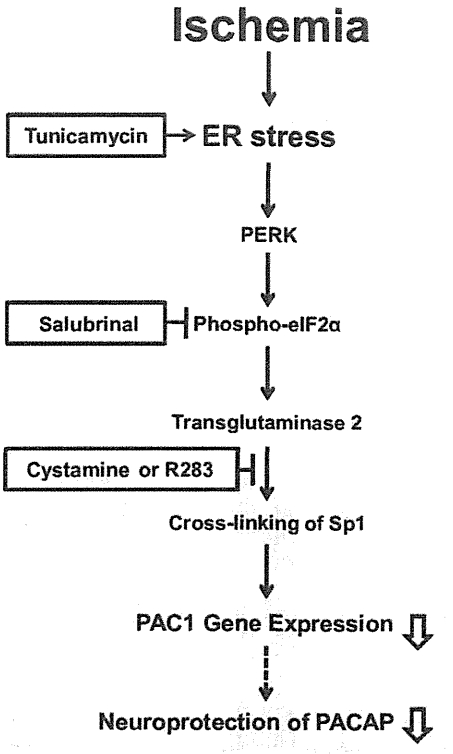

FIGURE 8. **Schematic diagram showing how suppression of PAC1 is induced by brain ischemia via ER stress-mediated PERK activation, resulting in cross-linking of Sp1 by TG2.**

cystamine (data not shown) in agreement with previous reports (14, 15, 17, 24, 30, 31). The present finding that CHOP, GRP78, and cleaved caspase-3 were attenuated by the pretreatment with cystamine supports the previous report that the downstream activity of TG2 activates the calpain/caspase pathway (32). Also, knocking down of *TG2* expression significantly attenuated their cell death (data not shown), In fact, it was reported previously that infarct volumes in *TG2*-knockout mice were significantly smaller compared with those in wild type mice (33), suggesting that TG2 is a potential target for development of therapeutics of brain ischemia.

In conclusion, we have shown that ischemia-induced activation of the PERK pathway of ER stress, subsequently activating TG2 and cross-linking Sp1, results in the suppression of *PAC1* gene expression (Fig. 8), suggesting the attenuation of PACAP neuroprotection in brain ischemia. However, it is well known that brain ischemia also induces gene expression of several neurotrophic factors including NGF (34). Recently, we demonstrated that NGF augmented *PAC1* gene expression through the activation of Sp1 via the Ras/MAPK pathway in PC12 cells (5). These observations suggest that *PAC1* gene expression might be primarily suppressed but secondarily augmented and that Sp1 might be a pivotal transcriptional element in not only positive but also negative regulation of PAC1 gene expression. Because our findings regarding the suppression of *PAC1* expression by TG2 were demonstrated only in *in vitro* models of neuronal apoptosis with OGD ischemia injury, further detailed analyses of the neurodegenerative pathway and also the protective pathway *in vivo* must lead us to the important

pathophysiological knowledge of TG2 and PACAP. PACAP is well known to exhibit potent neuroprotection and thus could be expected as a therapeutic drug for brain ischemia. The present finding that *PAC1* expression is suppressed by ischemia or ER stress should be substantially considered in the clinical application of a PAC1 agonist-like drug for effective treatment of ischemic damage following on stroke.

Acknowledgments—We thank Dr. Shrestha Rajan and Dr. Xian-Yang Qin for excellent technical assistance and helpful advice.

REFERENCES

1. Vaudry, D., Falluel-Morel, A., Bourgault, S., Basille, M., Burel, D., Wurtz, O., Fournier, A., Chow, B. K., Hashimoto, H., Galas, L., and Vaudry, H. (2009) Pituitary adenylate cyclase-activating polypeptide and its receptors: 20 years after the discovery. *Pharmacol. Rev.* **61,** 283–357
2. Uchida, D., Arimura, A., Somogyvári-Vigh, A., Shioda, S., and Banks, W. A. (1996) Prevention of ischemia-induced death of hippocampal neurons by pituitary adenylate cyclase-activating polypeptide. *Brain Res.* **736,** 280–286
3. Reglodi, D., Somogyvari-Vigh, A., Vigh, S., Maderdrut, J. L., and Arimura, A. (2000) Neuroprotective effects of PACAP38 in a rat model of transient focal ischemia under various experimental conditions. *Ann. N.Y. Acad. Sci.* **921,** 119–128
4. Riek-Burchardt, M., Kolodziej, A., Henrich-Noack, P., Reymann, K. G., Höllt, V., and Stumm, R. (2010) Differential regulation of CXCL12 and PACAP mRNA expression after focal and global ischemia. *Neuropharmacology* **58,** 199–207
5. Miura, A., Odahara, N., Tominaga, A., Inoue, K., Kambe, Y., Kurihara, T., and Miyata, A. (2012) Regulatory mechanism of PAC1 gene expression via Sp1 by nerve growth factor in PC12 cells. *FEBS Lett.* **586,** 1731–1735
6. Yeh, S. H., Yang, W. B., Gean, P. W., Hsu, C. Y., Tseng, J. T., Su, T. P., Chang, W. C., and Hung, J. J. (2011) Translational and transcriptional control of Sp1 against ischaemia through a hydrogen peroxide-activated internal ribosomal entry site pathway. *Nucleic Acids Res.* **39,** 5412–5423
7. Lee, J., Kosaras, B., Aleyasin, H., Han, J. A., Park, D. S., Ratan, R. R., Kowall, N. W., Ferrante, R. J., Lee, S. W., and Ryu, H. (2006) Role of cyclooxygenase-2 induction by transcription factor Sp1 and Sp3 in neuronal oxidative and DNA damage response. *FASEB J.* **20,** 2375–2377
8. Ryu, H., Lee, J., Zaman, K., Kubilis, J., Ferrante, R. J., Ross, B. D., Neve, R., and Ratan, R. R. (2003) Sp1 and Sp3 are oxidative stress-inducible, antideath transcription factors in cortical neurons. *J. Neurosci.* **23,** 3597–3606
9. Lee, M., Bikram, M., Oh, S., Bull, D. A., and Kim, S. W. (2004) Sp1-dependent regulation of the RTP801 promoter and its application to hypoxia-inducible VEGF plasmid for ischemic disease. *Pharm. Res.* **21,** 736–741
10. Miki, N., Ikuta, M., and Matsui, T. (2004) Hypoxia-induced activation of the retinoic acid receptor-related orphan receptor α4 gene by an interaction between hypoxia-inducible factor-1 and Sp1. *J. Biol. Chem.* **279,** 15025–15031
11. Hayashi, T., Saito, A., Okuno, S., Ferrand-Drake, M., Dodd, R. L., and Chan, P. H. (2004) Oxidative injury to the endoplasmic reticulum in mouse brains after transient focal ischemia. *Neurobiol. Dis.* **15,** 229–239
12. Szegezdi, E., Fitzgerald, U., and Samali, A. (2003) Caspase-12 and ER stress-mediated apoptosis: the story so far. *Ann. N.Y. Acad. Sci.* **1010,** 186–194
13. Tominaga, A., Sugawara, H., Inoue, K., and Miyata, A. (2008) Implication of pituitary adenylate cyclase-activating polypeptide (PACAP) for neuroprotection of nicotinic acetylcholine receptor signaling in PC12 cells. *J. Mol. Neurosci.* **36,** 73–78
14. Boyce, M., Bryant, K. F., Jousse, C., Long, K., Harding, H. P., Scheuner, D., Kaufman, R. J., Ma, D., Coen, D. M., Ron, D., and Yuan, J. (2005) A selective inhibitor of eIF2α dephosphorylation protects cells from ER stress. *Science* **307,** 935–939
15. Nakka, V. P., Gusain, A., and Raghubir, R. (2010) Endoplasmic reticulum stress plays critical role in brain damage after cerebral ischemia/reperfusion in rats. *Neurotox. Res.* **17,** 189–202
16. Caccamo, D., Campisi, A., Currò, M., Li Volti, G., Vanella, A., and Ientile, R. (2004) Excitotoxic and post-ischemic neurodegeneration: involvement of transglutaminases. *Amino Acids* **27,** 373-379
17. Ientile, R., Caccamo, D., Marciano, M. C., Currò, M., Mannucci, C., Campisi, A., and Calapai, G. (2004) Transglutaminase activity and transglutaminase mRNA transcripts in gerbil brain ischemia. *Neurosci. Lett.* **363,** 173–177
18. Tolentino, P. J., Waghray, A., Wang, K. K., and Hayes, R. L. (2004) Increased expression of tissue-type transglutaminase following middle cerebral artery occlusion in rats. *J. Neurochem.* **89,** 1301-1307
19. Lorand, L., and Graham, R. M. (2003) Transglutaminases: cross-linking enzymes with pleiotropic functions. *Nat. Rev. Mol. Cell Biol.* **4,** 140–156
20. Verhaar, R., Drukarch, B., Bol, J. G., Jongenelen, C. A., Musters, R. J., and Wilhelmus, M. M. (2012) Increase in endoplasmic reticulum-associated tissue transglutaminase and enzymatic activation in a cellular model of Parkinson's disease. *Neurobiol. Dis.* **45,** 839–850
21. Tatsukawa, H., Fukaya, Y., Frampton, G., Martinez-Fuentes, A., Suzuki, K., Kuo, T. F., Nagatsuma, K., Shimokado, K., Okuno, M., Wu, J., Iismaa, S., Matsuura, T., Tsukamoto, H., Zern, M. A., Graham, R. M., and Kojima, S. (2009) Role of transglutaminase 2 in liver injury via cross-linking and silencing of transcription factor Sp1. *Gastroenterology* **136,** 1783–1795
22. Tatsukawa, H., Sano, T., Fukaya, Y., Ishibashi, N., Watanabe, M., Okuno, M., Moriwaki, H., and Kojima, S. (2011) Dual induction of caspase 3- and transglutaminase-dependent apoptosis by acyclic retinoid in hepatocellular carcinoma cells. *Mol. Cancer* **10,** 4
23. Kuo, T. F., Tatsukawa, H., Matsuura, T., Nagatsuma, K., Hirose, S., and Kojima, S. (2012) Free fatty acids induce transglutaminase 2-dependent apoptosis in hepatocytes via ER stress-stimulated PERK pathways. *J. Cell. Physiol.* **227,** 1130–1137
24. Currò, M., Condello, S., Caccamo, D., Ferlazzo, N., Parisi, G., and Ientile, R. (2009) Homocysteine-induced toxicity increases TG2 expression in Neuro2a cells. *Amino Acids* **36,** 725–730
25. Griffin, M., Mongeot, A., Collighan, R., Saint, R. E., Jones, R. A., Coutts, I. G., and Rathbone, D. L. (2008) Synthesis of potent water-soluble tissue transglutaminase inhibitors. *Bioorg. Med. Chem. Lett.* **18,** 5559–5562
26. Skill, N. J., Johnson, T. S., Coutts, I. G., Saint, R. E., Fisher, M., Huang, L., El Nahas, A. M., Collighan, R. J., and Griffin, M. (2004) Inhibition of transglutaminase activity reduces extracellular matrix accumulation induced by high glucose levels in proximal tubular epithelial cells. *J. Biol. Chem.* **279,** 47754–47762
27. Kambe, Y., and Miyata, A. (2012) Role of mitochondrial activation in PACAP-dependent neurite outgrowth. *J. Mol. Neurosci.* **48,** 550–557
28. Hoffmann, A., Ciani, E., Houssami, S., Brabet, P., Journot, L., and Spengler, D. (1998) Induction of type I PACAP receptor expression by the new zinc finger protein Zac1and p53. *Ann. N.Y. Acad. Sci.* **11,** 49–58
29. Ressler, K. J., Mercer, K. B., Bradley, B., Jovanovic, T., Mahan, A., Kerley, K., Norrholm, S. D., Kilaru, V., Smith, A. K., Myers, A. J., Ramirez, M., Engel, A., Hammack, S. E., Toufexis, D., Braas, K. M., Binder, E. B., and May, V. (2011) Post-traumatic stress disorder is associated with PACAP and the PAC1 receptor. *Nature* **470,** 492–497
30. Woo, S. K., Kwon, M. S., Geng, Z., Chen, Z., Ivanov, A., Bhatta, S., Gerzanich, V., and Simard, J. M. (2012) Sequential activation of hypoxia-inducible factor 1 and specificity protein 1 is required for hypoxia-induced transcriptional stimulation of Abcc8. *J. Cereb. Blood Flow Metab.* **32,** 525–536
31. Shin, D. M., Kang, J., Ha, J., Kang, H. S., Park, S. C., Kim, I. G., and Kim, S. J. (2008) Cystamine prevents ischemia-reperfusion injury by inhibiting polyamination of RhoA. *Biochem. Biophys. Res. Commun.* **365,** 509–514
32. Yoo, J. O., Lim, Y. C., Kim, Y. M., and Ha, K. S. (2012) Transglutaminase 2 promotes both caspase-dependent and caspase-independent apoptotic cell death via the calpain/Bax protein signaling pathway. *J. Biol. Chem.* **287,** 14377–14388
33. Colak, G., and Johnson, G. V. (2012) Complete transglutaminase 2 ablation results in reduced stroke volumes and astrocytes that exhibit increased survival in response to ischemia. *Neurobiol. Dis.* **45,** 1042–1050
34. Lee, T. H., Kato, H., Chen, S. T., Kogure, K., and Itoyama, Y. (1998) Expression of nerve growth factor and trkA after transient focal cerebral ischemia in rats. *Stroke* **29,** 1687–1696

Cell

RNA-Methylation-Dependent RNA Processing Controls the Speed of the Circadian Clock

Jean-Michel Fustin,[1] Masao Doi,[1] Yoshiaki Yamaguchi,[1] Hayashi Hida,[1] Shinichi Nishimura,[2] Minoru Yoshida,[3] Takayuki Isagawa,[4] Masaki Suimye Morioka,[4] Hideaki Kakeya,[2] Ichiro Manabe,[4] and Hitoshi Okamura[1,*]

[1]Graduate School of Pharmaceutical Sciences, Department of System Biology, Kyoto University, 46-29 Yoshida-Shimo-Adachi-cho, Sakyo-ku, Kyoto 606-8501, Japan

[2]Graduate School of Pharmaceutical Sciences, Department of System Chemotherapy and Molecular Sciences, Kyoto University, 46-29 Yoshida-Shimo-Adachi-cho, Sakyo-ku, Kyoto 606-8501, Japan

[3]Chemical Genetics Laboratory, RIKEN, Hirosawa 2-1, Wako, Saitama 351-0198, Japan

[4]The University of Tokyo, Graduate School of Medicine, Department of Cardiovascular Medicine, 7-3-1 Hongo, Bunkyo, Tokyo 113-8655, Japan

*Correspondence: okamurah@pharm.kyoto-u.ac.jp

http://dx.doi.org/10.1016/j.cell.2013.10.026

SUMMARY

The eukaryotic biological clock involves a negative transcription-translation feedback loop in which clock genes regulate their own transcription and that of output genes of metabolic significance. While around 10% of the liver transcriptome is rhythmic, only about a fifth is driven by de novo transcription, indicating mRNA processing is a major circadian component. Here, we report that inhibition of transmethylation reactions elongates the circadian period. RNA sequencing then reveals methylation inhibition causes widespread changes in the transcription of the RNA processing machinery, associated with m^6A-RNA methylation. We identify m^6A sites on many clock gene transcripts and show that specific inhibition of m^6A methylation by silencing of the m^6A methylase *Mettl3* is sufficient to elicit circadian period elongation and RNA processing delay. Analysis of the circadian nucleocytoplasmic distribution of clock genes *Per2* and *Arntl* then revealed an uncoupling between steady-state pre-mRNA and cytoplasmic mRNA rhythms when m^6A methylation is inhibited.

INTRODUCTION

The mammalian circadian clock regulates metabolism mainly via transcriptional control of clock output genes coding for master metabolic switches or rate-limiting enzymes. Metabolism in turn can adjust the clock, for example by modulating acetylation/deacetylation of histones on promoters activated by core clock protein complex CLOCK:ARNTL (Nakahata et al., 2008) or directly by affecting acetylation status of PER proteins (Asher et al., 2008).

(De)acetylations, however, are only one of many possible biochemical modifications that have the potential to link the circadian clock with metabolism. Here, we focused on transmethylations, i.e., the addition of only one carbon ($-CH_3$) to target substrates. Unlike acetylation that only affects proteins, transmethylations are found at each step of the central dogma: DNA methylation, RNA methylation, and protein methylation (histone and nonhistone) have all been described (Carmel and Jacobsen, 2001). The role of histone methylation for the function of the circadian clock in mammals has recently been investigated (Katada and Sassone-Corsi, 2010; Valekunja et al., 2013; Vollmers et al., 2012). Similarly, the significance of the less dynamic DNA CpG methylation for circadian clock inactivation during the development of cancer and other diseases has been suggested (Ripperger and Merrow, 2011). In contrast, the role of nonhistone protein methylation and RNA methylation is unknown.

It has been known for many years that about 10% of genes are rhythmic in the liver, driven by the circadian clock (Akhtar et al., 2002). More recent RNA-sequencing data have shown that, of these rhythmic genes, only about a fifth is driven by de novo transcription (Koike et al., 2012). This observation has put regulation of splicing and RNA processing at the forefront of biology since it is not only significant for the function of the clock itself but also how it regulates metabolism. In this light, RNA-methylation-dependent RNA processing appears to be an interesting avenue.

All transmethylations, to various degrees, are influenced by the metabolic state of the cell due to their sensitivity to the availability of S-adenosylmethionine (SAM), the universal methyl donor cosubstrate, and to the relative amount of the its by-product, S-adenosylhomocysteine (SAH), that acts as a competitive inhibitor (Carmel and Jacobsen, 2001). The SAM/SAH ratio is known as the "methylation potential." Investigations into cellular transmethylations have relied on the pharmacological inhibition of SAH hydrolysis (Chiang, 1998). This inhibition leads to the accumulation of SAH, the decrease of the methylation potential, and ultimately to the inhibition of transmethylations.

To our knowledge, this approach has never been applied to the investigation of which transmethylations are needed for the circadian clock function. Here, we report that the mammalian circadian clock is exquisitely sensitive to the biochemical inhibition